Aging in the LHCb Outer Tracker

Ivan Mous

Master thesis

Vrije Universiteit
Faculteit der Exacte Wetenschappen
Particle- and astroparticle physics master
De Boelelaan 1081a
1081 HV Amsterdam

Research performed at:
NIKHEF
Kruislaan 409
1098 SJ Amsterdam

November 2007

Special thanks to dr. N Tuning

Abstract

The detector modules of the LHCb Outer Tracker have shown to suffer from gain loss after irradiation. This process is referred to as aging. The purpose of this thesis is to study and to try to solve this problem. We have analyzed the parameters that affect the aging, and compared our aging effects with those seen in other experiments. Using a special chamber, we were also able to determine that the glue used in the construction of the OT modules cause the aging. We have tested several possible solutions to the aging problem. Extensive flushing, low gas flow during operation, the addition of oxygen to the counting gas, high voltage training of the anode wires, and finally heating of the modules all showed beneficial effects. Further research will be necessary to investigate the long term behavior.

Contents

1 Introduction **5**
- 1.1 LHCb . . . 5
  - 1.1.1 Objectives of LHCb . . . 5
  - 1.1.2 LHCb design overview . . . 6
- 1.2 Overview of the Outer Tracker . . . 7
- 1.3 The aging problem . . . 7

2 The Outer Tracker **11**
- 2.1 Drift chambers . . . 11
- 2.2 Outer Tracker specifications . . . 12
- 2.3 Expected irradiation for the Outer Tracker . . . 16

3 Introduction to aging **19**
- 3.1 Carbon deposits . . . 19
- 3.2 Silicon . . . 21
- 3.3 Malter effect . . . 22
- 3.4 Wire damage . . . 23
- 3.5 Summary . . . 24

4 Aging analysis **25**
- 4.1 Earlier aging tests . . . 25
- 4.2 Description of the observed gain loss . . . 27
  - 4.2.1 Wire inspection . . . 33
  - 4.2.2 Quantitative aging measurement . . . 34
- 4.3 Aging parameters . . . 35
  - 4.3.1 Collected charge and intensity . . . 35
  - 4.3.2 Time . . . 39
  - 4.3.3 Gas flow . . . 42
  - 4.3.4 Position . . . 42
  - 4.3.5 Voltage . . . 44
  - 4.3.6 Radiation . . . 45
  - 4.3.7 Space charge . . . 46
- 4.4 Summary . . . 49

5 Previous experiments **51**
5.1 Intensity dependence tests 51
5.2 HERA-B Outer Tracker 53
5.3 ATLAS Transition Radiation Tracker 54
5.4 COMPASS Large Area Tracker 54
5.5 CDF Central Outer Tracker 55
5.6 CMS Muon Chamber 56
5.7 Summary 57

6 The cause of the aging **59**
6.1 Openable chamber 59
6.2 Straws and gas mixture 60
6.3 Panel 61
6.4 Glue 62
6.5 Summary 64

7 Solutions **65**
7.1 Flushing 65
7.2 Heating 66
7.3 HV training 70
7.4 Oxygen 73
7.5 Summary 75

8 Conclusion **77**

Chapter 1

Introduction

The goal of this thesis is to investigate, and if possible solve, the aging problem that the Outer Tracker modules have been found to experience. The Outer Tracker modules are designed as a part of the LHCb experiment, which is in turn a part of the Large Hadron Collider project. We shall discuss the LHCb and its goals, before turning to the Outer Tracker and our problems.

1.1 LHCb

The LHCb experiment is one of the four experiments constructed around the Large Hadron Collider [1]. This particle accelerator, with a proton beam energy of 7 TeV, is currently being constructed at CERN near Geneva.

1.1.1 Objectives of LHCb

The LHC is expected to create a large amount of B (anti-)mesons. The LHCb experiment is designed to study the decays of these B mesons, and more specifically to investigate CP violating effects in these decays.

Charge-Parity symmetry implies that the transition amplitude is unchanged after a parity operation (inverting the spatial coordinates) and a charge operation (replacing the particles by their anti-particles). The hypothesis that there is no difference between those decays is referred to as CP symmetry. CP symmetry was proposed after it was discovered that Charge [2] and Parity [3] symmetry separately were maximally violated (one of the two decays never occurs in nature) in weak decays, reflected by the fact that right-handed neutrinos are not observed in nature. However, the combined CP symmetry seemed to be valid. But in 1964, it was discovered that CP symmetry is in fact violated in the neutral Kaon system [4].

The existence of CP violation means that there is a fundamental difference between matter and antimatter. The existence of CP violation is one of the necessary components of the theory [5] to explain why the universe appears to be dominated by matter[1]. The CKM matrix in the standard model of physics

[1] Although the current data on the magnitude of CP violation suggest that the violation effect is too small to explain the current composition of the universe

(see [6, 7] for more details) indeed allows for CP symmetry violation in weak interactions involving quarks from different generations. Both the neutral Kaon (which contains a 1st generation d quark and a 2nd generation s quark) and the B-meson (which contains a 3rd generation b quark and one 1st or 2nd generation quark) could therefore exhibit CP violation.

Early CP violation experiments have investigated the Kaon system, as the light Kaon mesons are relatively easy to create. The investigation of B mesons has several advantages over Kaons, such as the relatively long lifetime, the higher degree of CP violation (especially for B_d mesons), and the sensitivity to 'new physics', undiscovered particles that could have a measurable effect on neutral B mesons. Several experiments with B-mesons have been performed at so-called B-factory experiments, like BaBar [8] and Belle [9], where CP violation in the B-system was first observed. However, the high luminosity and the large $b\bar{b}$ cross section (due to the high beam energy) at the LHC will allow the LHCb experiment to measure a larger amount of B-mesons than previous experiments. In addition, the heavier B_s mesons will also be produced at LHC, in contrast to the existing experiments at the B-factories.

1.1.2 LHCb design overview

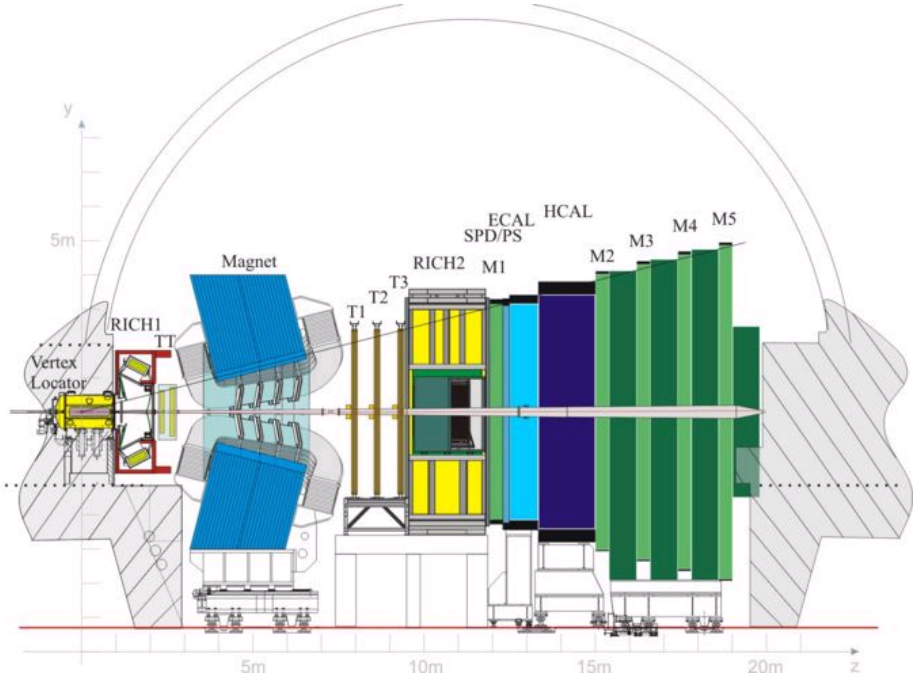

Figure 1.1: *A schematic picture of the LHCb experiment [10].*

Figure 1.1 shows a schematic picture of the LHCb spectrometer. The LHC beam pipe is shown extending along the z direction. The beam collisions occur in the vertex locator, shown at the left of Fig. 1.1. Simulations have shown that most of the particles we are interested in measuring will move in the forward

direction (see also section 2.3). Therefore, the LHCb experiment is build as a single arm spectrometer, and not around the interaction point like, for instance, the ATLAS experiment.

The purpose of the vertex locator is to measure how far the B mesons traveled before decaying. From this information, the lifetime can be reconstructed. The two RICH detectors are Cherenkov detectors that are used to determine the velocity of passing particles, such as the decay products of the B mesons. The Trigger Tracker and the Inner/Outer Tracker (marked as T1, T2 and T3) are used to determine the momentum of passing particles. Combining this with the information on the velocity of these particles, we can determine the mass of the particles. The calorimeters are used to determine the energy of all particles, including the neutral particles, but excluding the muons. Their energy is determined with the muon chambers.

For a more detailed description of the LHCb experiment, see [10].

1.2 Overview of the Outer Tracker

As stated in section 1.1, the Outer Tracker (OT) is part of the system in the LHCb that determines the momentum of the charged particles that pass through the detectors. Charged particles moving through a uniform magnetic field will follow a circular path, where the radius of the circle depends on the momentum. In LHCb, the path of the particles are determined before and after they enter the field created by the magnet shown in Fig. 1.1. By fitting the particle tracks based on the locations where the particles passed though the VELO and the Trigger Tracker before the magnetic field, and through the Outer Tracker stations behind the magnet, the momentum can be extracted.

Figure 1.2 shows two F modules of the LHCb OT in a so-called C-frame, similar to the frames used in the actual setup. The two modules are placed in different layers in this picture. Two C-frames are placed on either side of the beam pipe, such that one full layer contains 14 F modules, and 8 smaller S modules. More details on the setup can be found in chapter 2.

As can be seen in Fig 1.2, the modules are placed vertically in the C-frames (along the y direction in Fig. 1.1). Because of the inherent properties of drift cell detectors (see section 2.1), the Outer Tracker has a high spatial resolution in the horizontal direction (the x direction in Fig. 1.1), perpendicular to the plane of the picture. This is exactly the direction we are interested in, since it is the same direction the magnet deflects charged particles into. The combined tracking system of the LHCb OT is designed and expected to be able to determine the momentum of passing particles with a resolution of $\frac{\delta p}{p} = 0.5\%$. This resolution will allow us to investigate the decay of B mesons by measuring the B-meson mass with high accuracy.

1.3 The aging problem

Originally, the Outer Tracker modules were designed to withstand a large irradiation dose during the planned 10 years of operation [11]. Tests with prototype

Figure 1.2: *Two LHCb Outer Tracker modules in two different layers in a C-Frame. In the actual LHCb setup, the Outer Tracker will consist of 12 C-frames, six on either side of the beampipe*

module indicated that this would be feasible with the chosen design (See section 4.1). These tests were performed at much higher intensities than we expect in the LHCb environment in order to accelerate the tests. This is the normal method of testing a detectors radiation hardness.

However, more recent tests have shown a very rapid gain loss of Outer Tracker modules under mild irradiation. Significant aging is found in a matter of days rather than years. In the LHC environment, this would result in a significantly reduced detector efficiency within a month of operation.

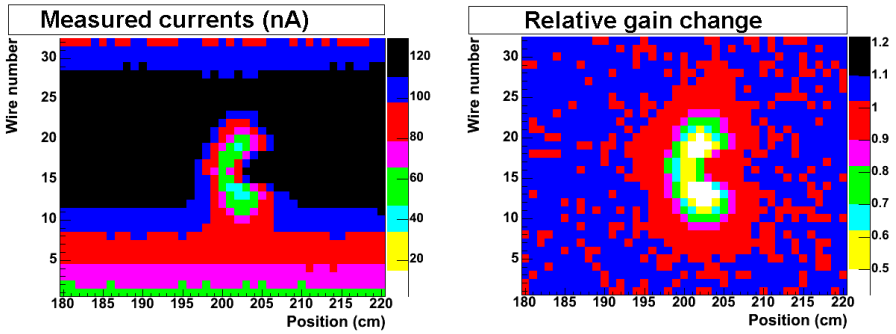

Figure 1.3: *An example of the gain loss observed after irradiation with a 2mCi ^{90}Sr (spherically symmetric) source. The left graph shows the current in nA (color scale) per wire (Y axis) when the scan source was at a given position (X axis). The right graph shows relative change of the detector response after irradiation. The gas flow goes from left to right. [Module 99, 23/04/2007]*

The aging pattern we observe has several unusual features, which can be seen in fig 1.3. These pictures show the absolute currents and relative gain loss (on the color scale) as a function of the position (on the x axis) for every wire (on the y axis). The aging is the result of 20 hours of irradiation with a point source placed above wire 16 at position 204 cm.

The aging pattern (the area where the currents are lower) has a crescent shape. Surprisingly, the gain loss is not the largest directly below the source, where the intensity is highest. Furthermore, the damage is not symmetric, since most of the damage appears to be left of the source position. Considering the gas flow, which goes from left to right in Fig. 1.3, this means most of the damage is upstream of the source. These two characteristics have been observed in almost all aging tests done with LHCb OT modules. Many other drift chamber detectors also experience aging effects in certain circumstances, but these characteristics have rarely been reported.

The objective of this thesis is to study the aging phenomena in the LHCb OT. We hope to gain at least a quantitative, and perhaps also a qualitative, understanding of the mechanisms behind the effect. Because of the adverse effects the aging could have on the LHCb performance, we also wish to find a remedy that can prevent or cure the aging effects. The LHCb OT modules have already been constructed. Therefore we are mostly interested in solutions that ensure good performance of these modules, rather than solutions that require

the construction of new modules.

Chapter 2

The Outer Tracker

In this chapter we shall discus the technical specifications of the LHCb Outer Tracker in greater detail. We will also look at simulations that specify what kind of radiation conditions the Outer Tracker can expect in the LHC environment.

2.1 Drift chambers

The Outer Tracker modules are drift-chamber detectors based on straw tube technology. Before going into the specifications of the Outer Tracker modules, we will first give an introduction to drift chambers in general.

A typical drift chamber contains an anode wire, a cathode and a drift gas. When a particle with sufficient energy passes through the drift gas it will ionize atoms or molecules in the gas. The electric field between the anode and the cathode pulls the resulting free electrons toward the anode wire. The electric field grows stronger closer to the center of the anode wire. This causes the electrons to accelerate, gaining kinetic energy. If the kinetic energy becomes larger than the ionization potential of the drift gas, these accelerated electrons can free more electrons. These electrons can again be accelerated and free additional electrons, causing an 'avalanche'. Note that for this to occur, the electrons must experience a large electric field over a sufficient distance before they reach the anode wire. Therefore, the applied voltage must be high and the anode wire must be thin.

Once the electrons have reached the anode wire, only the heavier and slower ions from the drift gas remain. These will be pulled toward the cathode. In the Outer Tracker, the cathode is a hollow cylindrical straw, with the anode wire in the center. The movement of the large number of charged particles in the gas around the wire causes a measurable electrical pulse in the anode wire. This pulse tells you that a particle passed through the detector.

The time between the passing of the particle and the detection of the pulse is a measure of the distance between the passing particle and the anode wire. The time of the passage of the particle is given by the LHC machine clock, since the collisions happen in bunches, and hence the drift time can be extracted. Knowing the drift velocity, this tells you at what distance from the anode wire the electrons were freed when the particle passed through the drift chamber.

The readout electronics is sensitive to the arrival of the first electrons, which means this technique will find the closest distance at which the particle passed the anode wire.

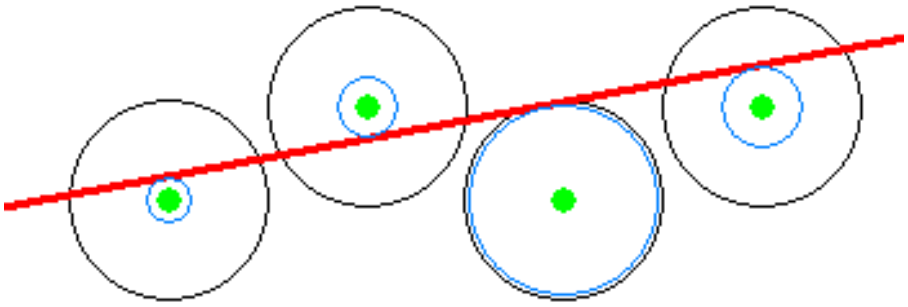

Figure 2.1: *An example of how four drift cell straws can be used to reconstruct a particle track. The distance between the particle track and the wire, as determined by the drift time, is indicated by the circles.*

Figure 2.1 shows how several cylindrical drift cells (like the Outer Tracker straws) can be used to reconstruct the particle track. The track, shown as a straight line, causes a signal in each of the four drift chamber cells. This signal will be delayed depending on how close the track came to the respective anode wires in the center of each drift cell. For each anode wire separately, this still gives an infinite number of possible passing points on a circle around the anode wire, since we do not know the direction of the passing particle. But by combining the distance information from all cells, we can fit and reconstruct the correct track. Note that the anode wire extends perpendicular to the plane shown in Fig. 2.1, and that the drift time gives no information on the distance at which the particle passes through in that direction. The high spatial resolution is only achieved in directions perpendicular to the anode wire.

For more information on drift chambers, see for example [12].

2.2 Outer Tracker specifications

In this section we want to give an overview of the technical specifications of the Outer Tracker. A more complete description can be found elsewhere [11, 13].

The anode wires used in the LHCb Outer Tracker are made of tungsten, with a gold layer. The tungsten provides good mechanical properties while the gold layer protects the wire from chemical reactions in the avalanche plasma. The diameter of the wire is 25 μm.

The straws consist of a inner winding of Kapton XC and an outer winding of aluminum foil, glued together with a 10 μm thick layer of polyester adhesive. Kapton XC, a carbon doped polyimide, was chosen because it proved to be resistant to (Malter) aging effects in high radiation environments, mechanically strong and easily available. The inner winding has a thickness of 40 μm. The aluminum outer layer shields the straw electrically, preventing cross talk. Cross

talk means that a particle passing through one straw causes signals in neighboring straws through electromagnetic interactions. The aluminum outer layer is 12 μm thick.

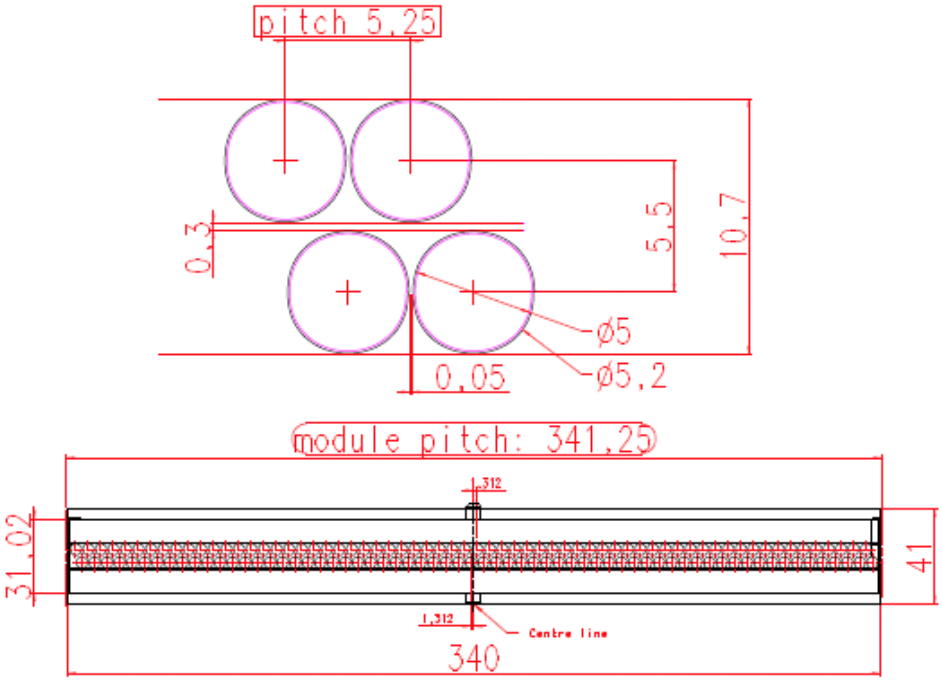

Figure 2.2: *The straw arrangement in an LHCb Outer Tracker module.*

The straws are organized in modules containing two staggered layers of straws. The arrangement and dimensions are shown in fig 2.2. Figure 2.3 shows the different kinds of modules used, and their arrangement in the LHCb Outer Tracker. The F modules are 493 cm long, and contain two staggered layers of straws, as shown in Fig. 2.2. The wires of both sets are not connected, and are read out separately at the top and bottom of the modules. The S1 and S2 modules are half the size of F modules and are located above and below the beam pipe. The S3 are only 32 straws wide. The gap in the middle of the module arrangement is the area where the particle density is predicted to be too large for the Outer Tracker. This is where the Inner Tracker will be placed. In the middle of the Inner Tracker the LHC beam pipe is placed.

All module types contain these layers of straws with the same structure. A 1 cm thick core of Rohacell foam, covered on both sides with a Carbon Fiber Composite, covers the broad side of the modules (above and below the straw layers in the lower part of fig 2.2). On the inside of these panels there is a thin laminate of Kapton and aluminum. The straws are glued to this laminate with Araldite AW 103. On the side of the modules (left and right of the straws in Fig. 2.2), aluminum plates coated with Kapton are placed. These seal the sides of the module and provide more mechanical stability to the module. F modules have an electronic readout system for the wires on both sides. The module is

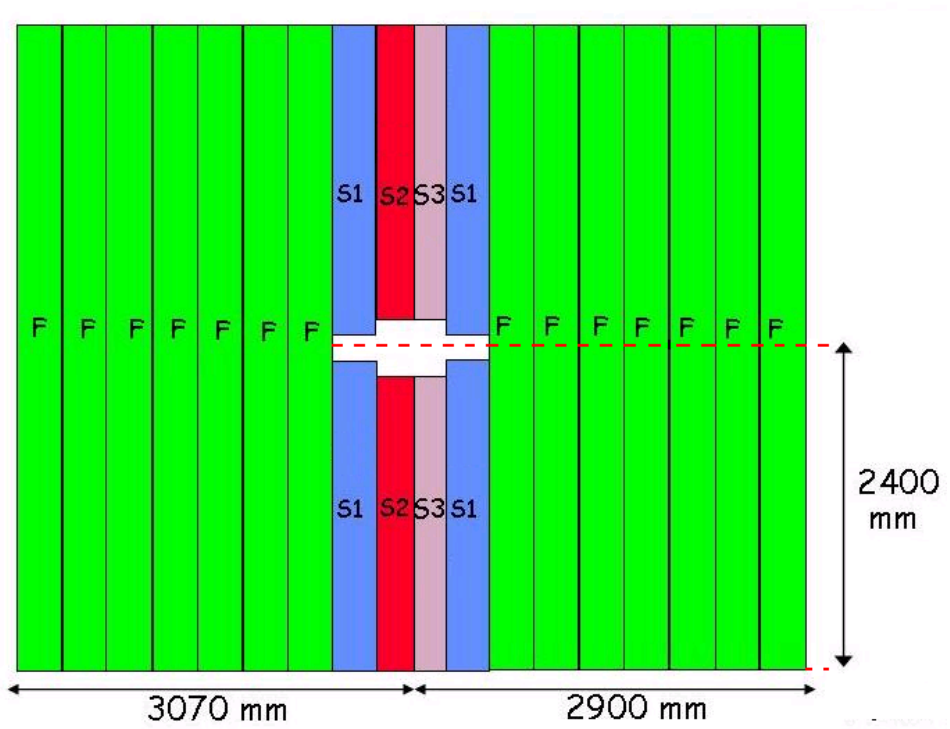

Figure 2.3: *The module arrangement of one layer of the LHCb Outer Tracker. The cross in the middle will be covered by the Inner Tracker detector. The beam pipe traverses the detectors in the center.*

fortified at those ends with an aluminum plate between the two foam layers. S modules only have a readout system at one end of the module. The other end (the end of the modules facing the gap in fig 2.3) is simply closed off. All modules have 4 gas pipes at both ends, to ensure a good gas flow throughout the module. All modules are 'stand-alone', meaning they provide their own mechanical stability, gas tightness and readout. In principle, a single module could be used as a (very small) detector station.

The modules are arranged in 3 stations each consisting of 4 layers of modules as shown in Fig. 2.4. Each layer is organized as shown in Fig. 2.3. In order to have a some ability to measure the y-coordinate at which a particle passes through a station, some of the module layers are placed at an angle. Two of the layers are suspended vertically, one layer is placed at a $+5°$ angle and one layer is placed at a $-5°$ angle.

An important choice for drift chambers is the choice of the drift gas (mixture). As explained in section 2.1, the detector relies on ionization of the drift gas. Therefore, we want a gas that has a low ionization potential and preferably cannot absorb energy in any other way (e.g. vibrational, rotational). The latter requirement means that atomic gasses are preferable. Halogens, particularly argon and xenon, are popular choices. Secondly, a gas component is required to absorb the photons, created in the avalanche, that do not have enough energy

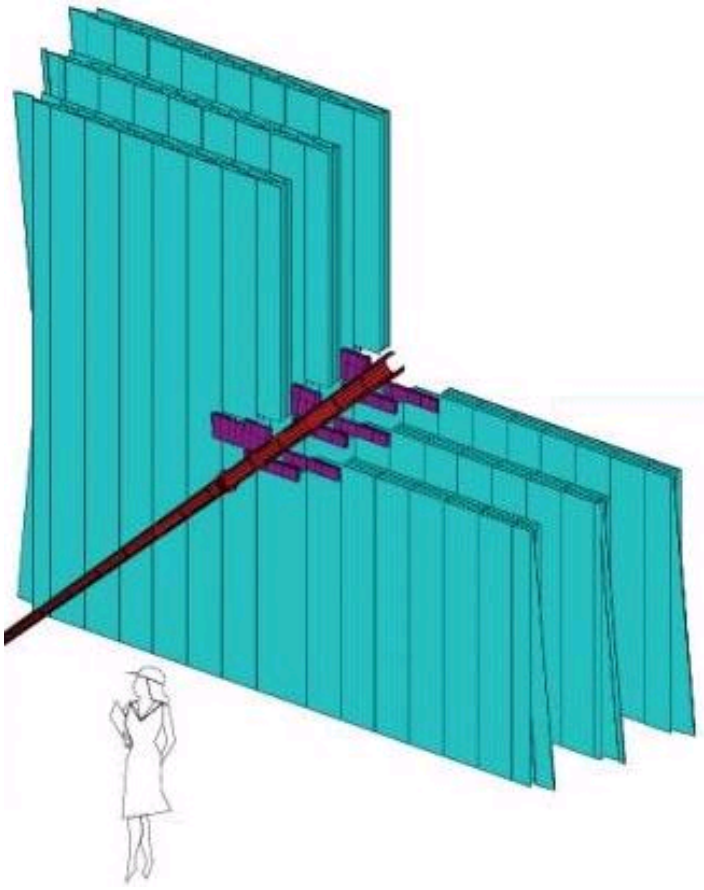

Figure 2.4: *The station arrangement in the LHCb Outer Tracker. Note that one quarter of the detector is not shown to make the other parts of the detector more visible.*

to ionize the gas. Otherwise, those photons will pass through the atomic gas and ionize the cathode. Another problem is that electrons accelerating toward the anode will experience many elastic collisions in a atomic gas, increasing the drift time. To solve these problems, a quencher gas is usually added. Popular choices include CH_4, CO_2 or DME.

Other gasses can be added to this mixture. A particular popular addition is CF_4. Gas mixture that contain some CF_4 have faster drift speeds. This is an advantage in high rate experiment, where the particles that need to be detected pass through at a high frequency. The LHC experiment certainly qualifies as high rate, as beam collisions occur every 25 ns. However, CF_4 can have adverse effects on the detector material. High rate irradiation tests showed that the CF_4 can etch the wire due to the presence of fluoride radicals (more on this in section 3.4). Therefore the Outer Tracker uses a 70/30 Ar/CO_2 mixture.

2.3 Expected irradiation for the Outer Tracker

Most of the aging effects in the Outer Tracker described in this report have been observe in laboratory tests. But of course, the aging effects in the actual LHC environment are more relevant. It is impossible to mimic an environment with such a high intensity of high energy hadronic particles in a small scale setup. Instead, we must extrapolate our results to the situation in the LHC. The radiation the Outer Tracker will receive during its operation has been simulated [14].

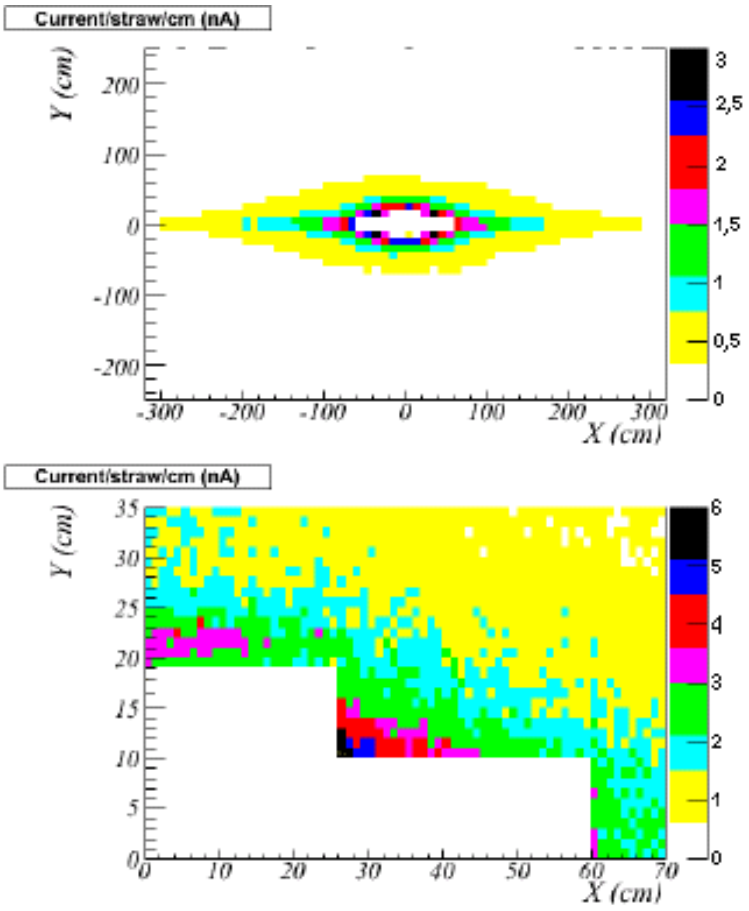

Figure 2.5: *The resulting current density per straw per centimeter at the LHCb Outer Tracker stations. The lower graph shows a zoom in of the first graph.*

Figure 2.5 shows the predicted current density per straw per wire at the Outer Tracker stations. It shows a 'frontal view' of the Outer tracker detector plane. The Outer tracker modules, and the straws, will extend along the Y direction. The plus-shaped white area in the middle of the graph shows the gap that will be in the actual Outer Tracker stations. Inside it will be the Inner Tracker and the LHC beam pipes.

As we can see from this graph, we expect currents of a few nA in a thin ring

around the beam pipe, and a broad area of currents of 1 nA and lower for a nominal operation at a luminosity of $2*10^{-37}$ $cm^{-2}s^{-1}$ with a gas gain of $2*10^4$. This latter area is far more stretched in the x direction, due to the orientation of the magnetic. As a result, we can expect all modules to experience currents around 0.5 nA/cm/wire at some point along the module. Some of the F modules can experience currents up to 3 nA/cm/wire, a few S modules might measure currents up to 6 nA/cm/wire.

The usual assumption of irradiation time in the LHC is that during one year there will be 10^7 seconds of irradiation. Under this assumption, the 'hottest' region in the Outer Tracker will receive a dose of 0.06 C/cm/wire per year, or 0.6 C/cm/wire during the planned 10 years of runtime. The LHCb OT was initially designed to withstand 2.5 C/cm/wire.

Chapter 3

Introduction to aging

In particle detection the term aging refers to a broad range of effects. A general definition of aging is the permanent decrease of the quality of a detector under the influence of irradiation. The particles that the detectors are designed to detect are also partly responsible for the irradiation that causes the aging. This means that it is not possible to simply shield the detector to prevent aging.

There is a large variety in causes and effects of aging. It is interesting to note that none of the major aging effects in wire chambers appear to be caused directly by the radiation. Reviews of various cases of aging in wire chambers [15, 16, 17] show that the causes of the aging effects can be found in the electron avalanche. The avalanche results in a large amount of kinetic energy being released in a small area surrounding the anode wire, resulting in an almost plasma-like state of the gas. As a result, molecular bonds will be broken in that region, leaving chemically reactive radicals in the gas. Some of these radicals will recombine into their original molecules, but some might also cause chemical reactions that are harmful to the operation of the detector. A consequence of this is that the chamber does not age while being irradiated if the voltage on the wires is turned off.

Although there exist theories about the mechanisms of all the methods of aging described in this chapter, little has been verified. Unfortunately, there is no real way to observe what exactly happens during the avalanches. The aging effect depends at least partly on chemical processes that occur inside the small avalanche region. The effects the aging has on the electric signals as measured by the readout system can be seen during operation. Our information of these mechanisms comes from removing and investigating parts of the detector (usually the wires) after the aging took place. We can then try to reconstruct the mechanisms based on the effects it has had on the detector material. But some degree of uncertainty about the mechanisms will remain.

3.1 Carbon deposits

One of the potentially dangerous effects is the formation of polymers. Any gas molecule that contain carbon atoms might be broken in the avalanche region. The resulting 'loose' carbon atoms are highly reactive, and can form bonds with

other free carbon atoms in the gas. The resulting molecule could again bind other carbon atoms, forming long polymers. At some point, the molecules will be too large to remain in a gas state and can form a solid deposit on the anode wire of the gas detector. Eventually, the anode wire can be coated by these deposits. An example of how a wire can be coated by deposits is shown in Fig. 3.1. The coating can either be conducting or insulating, but the detector performance is affected in either case.

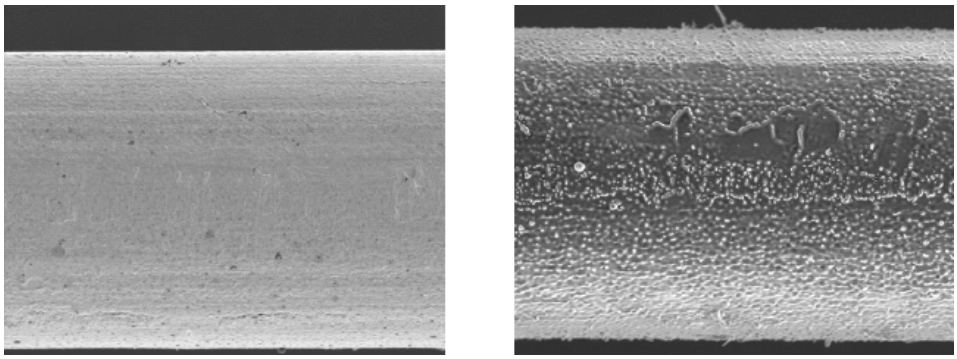

Figure 3.1: *A Scanning Electron Microscope image of a new (left) and an aged (right) wire from the CDF axial drift chambers [18]. See section 5.5 for more information on the CDF chamber.*

If the coating is insulating, the avalanche electrons will have difficulty reaching the anode wire. This can result in gain loss, signal distortion or sparking caused by the pile-up of charge around the wire. The effects of a conducting layer are less severe, but can still be significant. The main effect is that it makes the wire thicker, thereby lowering the gas gain. Also, the surface of the wire will become less regular, which may distort the signal.

The deposits may not always form a simple coating on the wires. In some cases, the deposits form so called whiskers, as shown in fig 3.2. It is believed that these are formed by discharges or sparks between the cathode and the anode. The spark causes some kind of damage to the anode wire, which primes that point for the creation of the whiskers. Since one cannot see the wire while the detector is operating, the creation itself of the whiskers is never observed. It is unknown if the whiskers themselves are created along the path of one or more of these sparks. However, it has been shown [15] that the whiskers only point in the direction where particles pass through.

Most carbon polymers contain several hydrogen atoms. As such, the risk of polymer deposits is largest if the gas used in the detector contains both carbon and hydrogen. An example is the use of CH_4 as the quenching gas. Methane used to be a popular choice as a quenching gas in low intensity experiments. But in the past few decades, as the intensity in experiments continued to increase, several experiments (such as [20, 21]) have reported severe aging effects with CH_4. Other quenching gases have replaced CH_4 in many experiments. However, using a different quenching gas does not guarantee protection from polymer formation. Most of the gas mixtures used in wire chamber contain some carbon

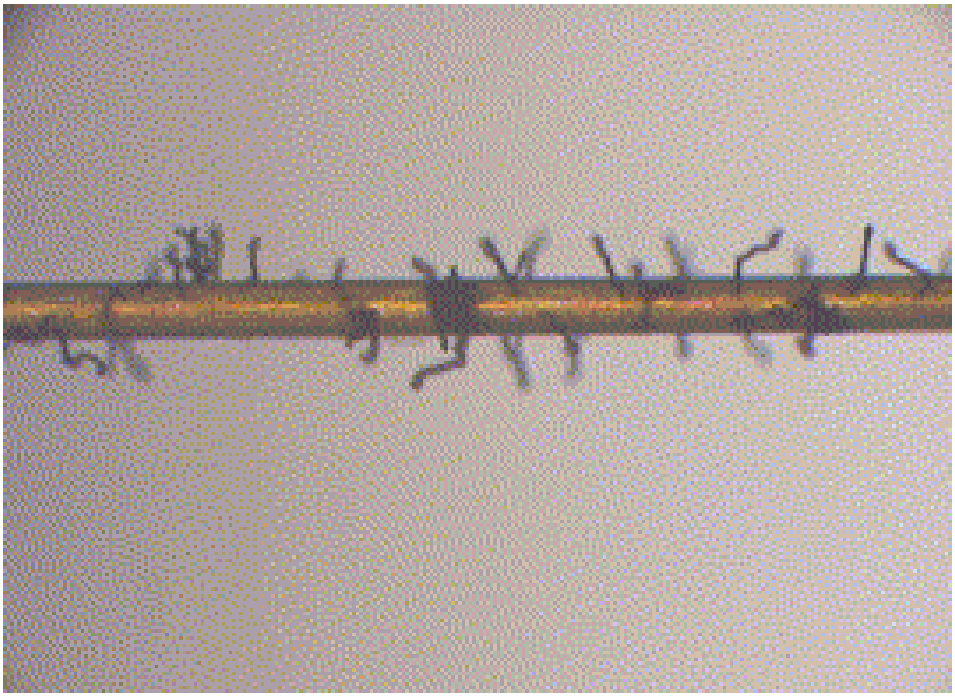

Figure 3.2: *An optical image of a wire from the HERA OTR [19].*

atoms, (CO_2, CF_4 and DME are all popular components) and the carbon can come from other sources than the gas itself, such as outgassing from certain glues, oils or certain parts of the gas system. On the other hand, having both carbon and hydrogen present does not always result in polymer formation. In fact, the addition of H_2O to gas mixtures that contain carbon is sometimes used to prevent polymer forming [19], since oxygen atoms from the H_2O molecules bind to carbon to form CO_2.

There seems to be no general solution to prevent polymer deposit formation. The cause and solution of polymer formation is not well understood, and appears to depend unpredictably on several parameters. Therefore possible solutions (adding H_2O, changing the gas mixture) should be tested before implementation.

3.2 Silicon

Silicon is a notorious cause of rapid aging in wire chambers. Experiments have shown that a gas containing a fraction of silicon as small as 10^{-12} can already cause significant aging in wire chambers [22]. Because its electron configuration is similar to that of carbon, it can form similar bonds. But because even small silicon molecules often form solid deposits while small carbon molecules remain in gaseous form, it is more dangerous than carbon. These deposits can cause very rapid gain drops. For these reasons, the use of silicon in wire chambers should always be avoided.

Unfortunately, it is widely used in (the production of) components of gas systems made by industrial manufacturers. Examples of components that can contain traces of silicon include [15] lubricants, adhesives, O-rings and gas flow regulators. Furthermore, there may be silicon pollution present in oils, polluted gas cylinders or as gas impurities. The presence of silicon is not always reported by the manufacturers if there are only tiny amounts present, or if silicon oil or lubricant was only used during manufacturing.

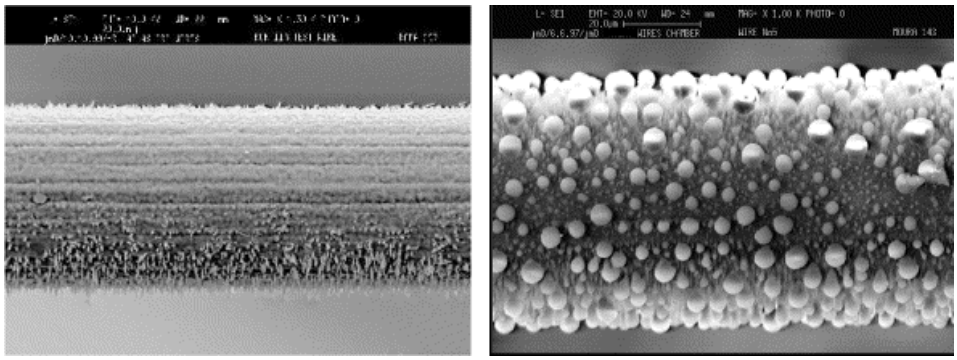

Figure 3.3: *Si deposits on the wires of the ATLAS TRT [23] (left) and the CMS muon chamber [24] (right), as seen with a SEM.*

Figure 3.3 shows a picture made with a scanning-tunneling electron microscope (SEM) of test wires from the ATLAS Trigger Tracker and the CMS muon chamber. Both wires are covered in silicon deposits, in the shape of tiny stakes and small blobs respectively. The source of the silicon contamination of the TRT was a lubricant used during the winding of the straw cathodes. In the CMS muon chamber, the silicon originated from the glue used to seal the modules.

There are two general ways to deal with silicon pollution. The first way is to simply remove the source of the pollution. Components from the gas system can be cleaned in an ultrasonic bath with isopropyl alcohol. If there is silicon contamination inside parts of the detector, those parts may need to be replaced [23]. The second method is adding a gas like CF_4 [24]. The fluoride radicals created in the avalanche can react with the silicon deposits. The reaction products can then (hopefully) be removed by the gas flow.

3.3 Malter effect

In 1936 L. Malter described how a the electric field caused by a large concentration positively charged ions can pull electrons out of a nearby surface [25]. In recent experiments such as HERA-B [19], the Malter effect has proven to cause aging of the cathode. It occurs if there are insulating deposits on the cathode tube (instead of the anode wire), or if the surface of the cathode itself becomes less conductive. Normally, deposits on the cathode are less of a problem since their surface area is so much larger than the surface of the wire. But

if a large enough area of the cathode is covered by deposits, the positive ions created in avalanches that drift toward the cathode cannot reach it. Instead, they pile up on top of the thin insulating coating from either the deposits or the damaged cathode material. This causes a strong electric field between the cathode and the ions. If the field is strong enough, it can pull electrons out of the cathode. These electrons can have enough kinetic energy to start their own avalanche. The ions resulting from these avalanches will again pile up, causing more electrons to be pulled out.

The result is a sustained current, whether there are particles passing through the straws or not. These currents remain until the high voltage on the wires is shut down. After turning the voltage back on, it will only take a few particle avalanches to regain the sustained currents. It is likely that the sustained currents will grow with time. If the cathode coating was created in the avalanche region, the constant avalanches caused by the Malter effect will produce more coating material. Eventually, one will see exponentially increasing currents. The most common way to fix a detector that suffers from the Malter effect is the addition of water vapor to the gas mixture. The water increases the conductivity of the damage cathodes.

3.4 Wire damage

Another form of aging is physical damage to the anode wires themselves. This occurs when radicals created in the avalanche are volatile enough to react with the anode material. An example would be oxygen radicals, which can bind with metal from the anode, causing it to rust.

A more common source of wire damage in gas detectors are fluoride radicals from CF_4. These radicals can react with the anode material, while the reaction products can be flushed away by the gas flow. This process is referred to as etching. [1]

Since etching requires chemical reactions with the anode, the risk of etching depends on the chemical properties of the anode material. Most straw tube gas detectors use gold plated wires. Since gold is a highly inert substance, it protects the wire core (usually tungsten) from etching.

However, even gold plated wires can suffer etching effects. During tests with prototypes of the LHCb Outer Tracker modules [26], a $Ar/CO_2/CF_4$ (75/10/15) mixture was used. Wires in the irradiated area proved to be highly susceptible to etching. Not only was the gold plating damaged after 0.6 C/cm of irradiation, but several wires broke in the irradiated area. Figure 3.4 shows a SEM picture of a broken and a wire with etching of the gold plating after irradiation. In contrast, the wires in the Ar/CO_2 (70/30) mixture showed no etching effects. This is the main reason that Ar/CO_2 was chosen as the gas mixture for the LHCb Outer Tracker.

[1] Note that the term etching is also used for the reaction with carbon or silicon deposits. This type of etching is actually beneficial to the detector lifetime. In this section, etching will refer to damage to the anode wire.

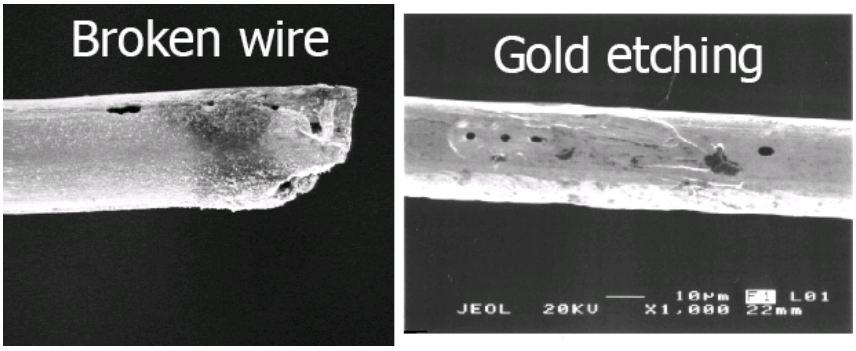

Figure 3.4: *SEM images of a broken wire, and a wire with damage to the gold plating, from an LHCb OT test module with $Ar/CO_2/CF_4$ (75/10/15) gas mixture.*

3.5 Summary

There is a broad variety of aging effects in gas detectors. The most common effects are formation of carbon or silicon deposits, wire etching and the Malter effect. Previous experiments have resulted in several possible solutions to prevent these effects. However, there is no solution to these problems that is guaranteed to work in all detectors. This is partly due to the fact that none of the effects can be directly observed as they happen, limiting our fundamental understanding. Before implementing any of the solutions in a large scale experiment, its effectiveness in that particular case should be experimentally verified.

Chapter 4

Aging analysis

Tests have shown that the LHCb OT modules suffer from significant decreases of the gas gain after several hours of irradiation. In this chapter, we shall discuss the features of this aging phenomenon. We will first discuss some of the aging tests performed prior to the mass construction of the modules. In section 4.2 we will show our way of detecting gain loss, as well as a more detailed description of the aging effects we observe. The analysis of aged wires, described in section 4.2.1, will show that the gain loss is due to carbon deposits on the anode wire. This type of aging has been discussed in section 3.1. We will also demonstrate our methods of quantifying the gain loss. Finally, we will show the effect of several parameters on the aging.

4.1 Earlier aging tests

The aging problem, in its current form, was discovered after production of the modules had been completed. But of course, the module design had been tested for aging effects prior to selecting the design for mass production. In this section we shall summarize the results of these aging tests with prototype modules:

- X-ray tests, with $Ar/CO_2/CF_4$ and Ar/CO_2 gas mixtures.
- Tests in the HERA-B experiment, with $Ar/CO_2/CF_4$.
- Proton tests, with $Ar/CH_4/CF_4$.
- β tests with Ar/CO_2.

The LHCb OT was originally intended to operate with $Ar/CO_2/CF_4$ mixture. The addition of CF_4 was deemed necessary to increase the electron drift time. As a result, many of the older tests have been performed with this mixture. However, a comparison study between Ar/CO_2 and $Ar/CO_2/CF_4$ [26, 27] showed stronger aging effects in the OT modules with CF_4. These tests were performed by irradiating a short test module with an X-ray tube. A 4 cm region was irradiated, receiving an intensity of about 1 μA/cm.

The straws containing $Ar/CO_2/CF_4$ showed several kinds of aging after less than 1 C/cm/wire. The effects included gain loss (even outside the irradiated

area), carbon deposits on the wire, wire etching and wire breaking. The straws with Ar/CO_2 did not show wire damage or gain loss as long as the water concentration in the gas was lower than 50 ppm. Optical inspection of the wire showed no changes in the irradiated area. A more detailed analysis did show some carbon and oxygen deposits, though these did not result in a gain loss.

The gain loss was measured by determining the pulse spectrum of a ^{55}Fe source along the wires, before and after the irradiation. Assuming that the investigated wire length was long enough, aging effects on the edges of the irradiated area should have been found if they were present.

The quoted irradiation intensity of 1 μA/cm is considerably higher than the intensities in our current experiments (<100nA/cm right below the source). The irradiation area was confined by a collimator. It is unknown exactly how quickly the intensity dropped outside the 4 cm area. It is thus not known if there was a broad area where the intensity was in the range of 1-10 nA/cm, which is where most damage is observed (See section 4.3.1). The exact reason as to why no aging was seen in this test remains unknown. Two of the more interesting aging tests done with the old CF_4 containing mixture are irradiations done with protons and inside the HERA-B experiment [28]. Creating usable hadronic radiation requires a lot more infrastructure and radiation safety measures than β or γ radiation. (Standard α radiation does not get through the straws.) During LHC operation hadrons will be a substantial part of the radiation the Outer Tracker receives. It is thus worth investigating if the Outer Tracker modules respond differently to hadronic radiation.

The proton test consisted of irradiating a single straw with a $Ar/CH_4/CF_4$ (74/6/20) with a 11 MeV proton beam. The wire received 130 mC/cm, with an intensity of 8 μA/cm. Although the test was primarily intended to test if the straws would suffer from the Malter effect, the possibility of anode aging was also tested. The results showed no evidence for either Malter effects or anode aging.

The test in HERA-B was performed with a prototype chamber, containing two layers of 32 straws. $Ar/CO_2/CF_4$ (65/5/30) was used as a drift gas. The chamber was placed near the interaction area of the HERA-B experiment. The setup was such that one side of the module (x=0) received a larger doses compared to the other end (x = 180 cm). The highest received irradiation dose is around 50 mC/cm. Figure 4.1 shows the results of scanning the module, as described in section 4.2. The currents in one wire is shown. There does not appear to be any difference between the scans done before (top) and after (bottom) the irradiation. It was concluded that the prototype was aging resistant.

The first evidence of aging in its current form was found in 2005 [29]. During a cross talk test, one wire was irradiated with a highly collimated ^{90}Sr source. The test was intended to investigate if electric pulses in the irradiated wire caused signals in the neighboring wires. But after the tests had been performed, the one irradiated wire showed a much lower gain at the irradiated spots. Figure 4.2 shows the currents measured in a scan (see section 4.2) along the irradiated wire 24 and its two nearest neighbors. All wires show two dips in the current, corresponding with the wire locators in the straws. But only wire 24 shows a large gain loss at the four irradiated positions, denoted by vertical bars in the

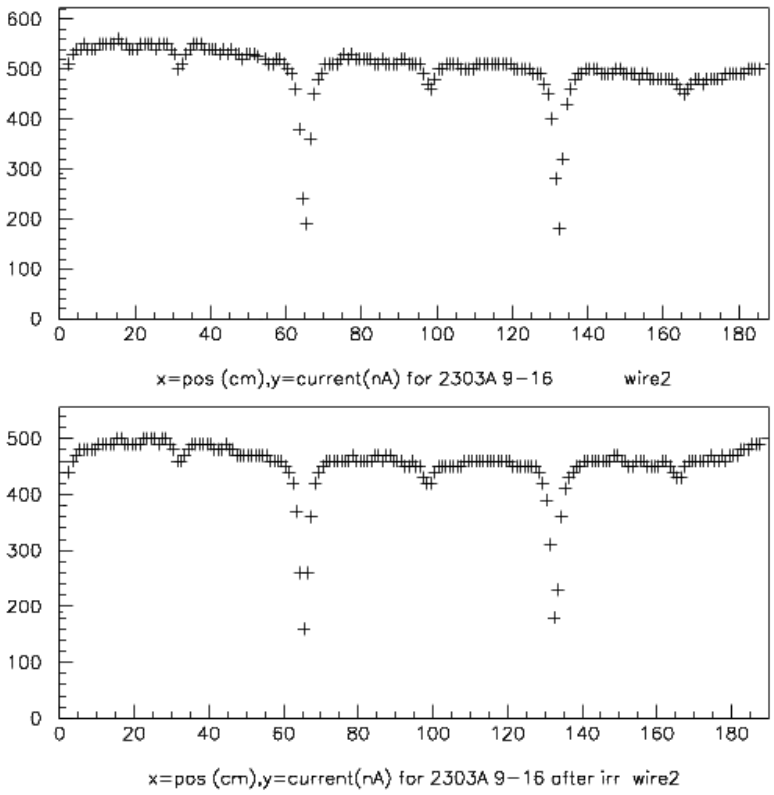

Figure 4.1: *The currents measured with a ^{90}Sr scan in one wire of the prototype module, before and after being irradiated in the HERA-B experiment. The area near x=0 received a much larger irradiation dose than the area near x=180 cm [28].*

graph.

By the time this problem was discovered and confirmed, construction of the Outer Tracker modules had already been completed. Since then a large number of aging tests have been performed to determine the cause of the aging, and to find a solution to the problem.

4.2 Description of the observed gain loss

In this section we shall treat the aging effects that we observe after a typical aging test. Our default aging tests is an irradiation for a period of 20 hours with a small, spherically symmetric 2mCi ^{90}Sr source. The gain along the entire length of the module is measured before and after the irradiation. A comparison between the measured detector response will show if the irradiation caused aging.

One could determine the gain of the module at a certain position with a monochromatic ^{55}Fe source. Photons from this source deposit a constant amount of energy in the detector. The gain can be obtained by comparing that

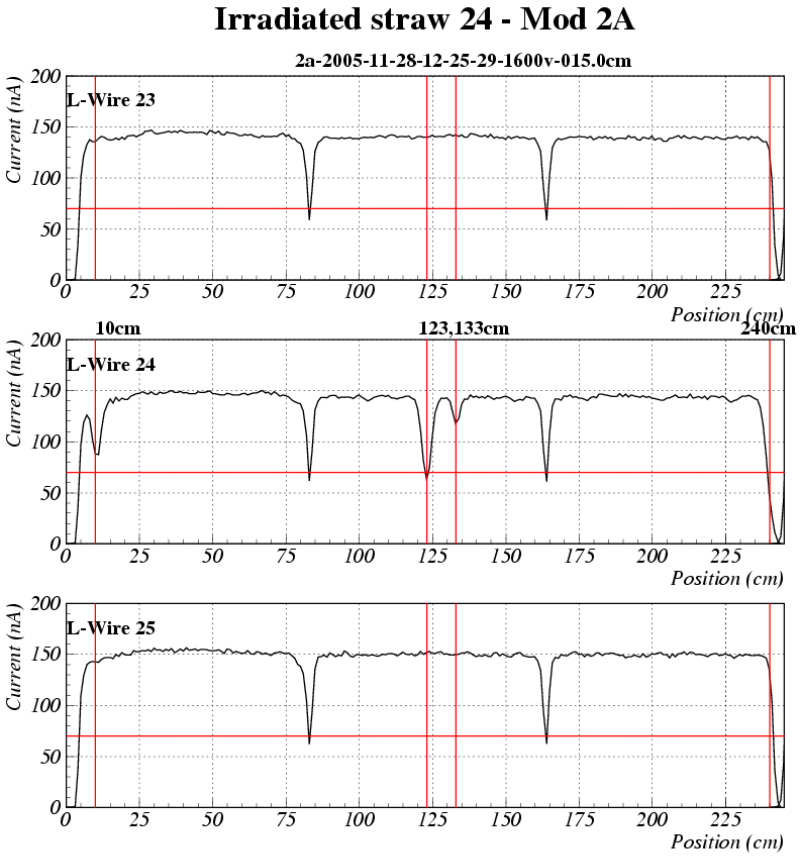

Figure 4.2: *The first documented case of aging seen with the current operating gas and parameters. Wire 24 has been irradiated at the locations denoted by the vertical bars. [Module 2, 06/06/2005]*

amount with the energy actually measured by the detector. In our setup, we prefer to measure the relative gain with an ^{90}Sr source. The source is placed over a certain area of the module for a fixed period of time. Instead of measuring the energy deposited by each particle, we measure the total energy deposited during a fixed time interval. This energy is measured as a current through the wire, which is proportional to the gain and the total amount of deposited energy. Since the time interval and the intensity of the source are constant, the current only depends on the gain, given that the wall thickness of the module is uniform.

Our setup is equipped with a 20 mCi ^{90}Sr source which is automatically moved along the module in steps of 1 cm. While the source scans the length of the module, the currents in all wires are written to a file in each step. This provides us with information about the relative gain at each position and in each wire of the module. For an optimal scan resolution with these 1cm steps, one would want a scanning source that irradiates a 1 cm wide area below it,

with a uniform irradiation density. No irradiation should be detectable outside of the 1 cm area. In practice, it is not possible to collimate a source in this manner. The scanning source in our setup has been experimentally verified to have a Gaussian irradiation profile, with a width of about 9.2 mm. As a result, around 70 % of the currents measured at any location of the scan source originates in the 1 cm area below it. This means that any gain variations along the wire length will appear slightly smeared out on the scan.

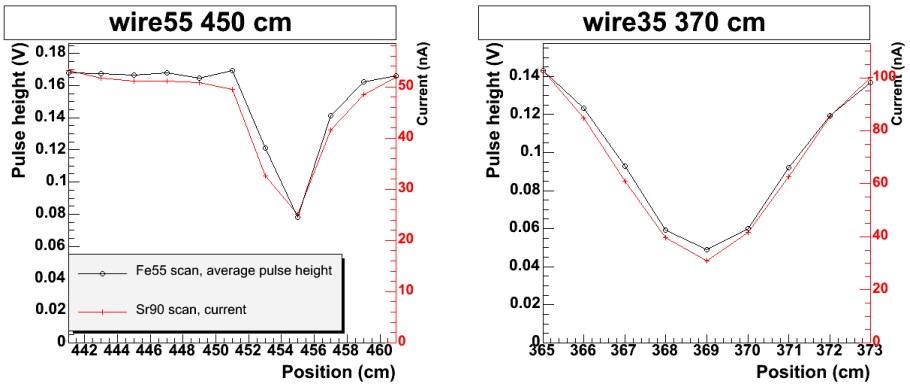

Figure 4.3: *The currents and average pulse heights measured per wire on a module with several areas with gain loss, measured with a ^{90}Sr and a ^{55}Fe scan respectively. [Module 30, 25/04/2007]*

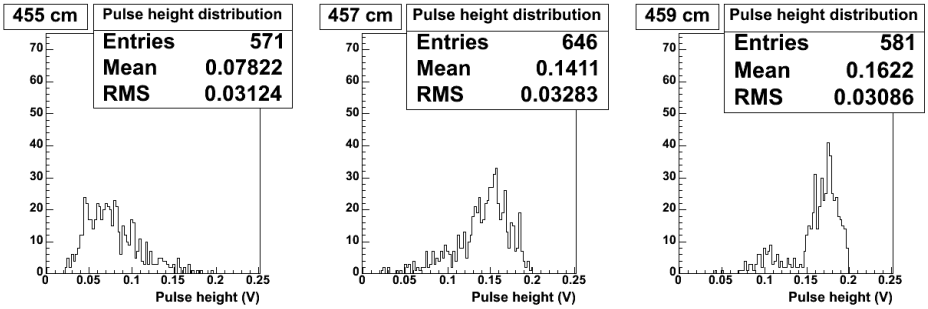

Figure 4.4: *The pulse height distributions corresponding to some of the positions in the ^{55}Fe scan shown in Fig. 4.3. Only pulse heights below 0.2 V could be measured, due to saturation of the preamplifier.*

To prove that our method measures gain loss in the same manner as the more common ^{55}Fe scan, we investigated an aged module with both methods. Figure 4.3 shows the currents from the ^{90}Sr scan and the average pulse heights of the ^{55}Fe scan measured in a single wire as a function of position. As we can see, the lower currents measured with the ^{90}Sr are indeed caused by a gain loss as measured with the ^{55}Fe method. The pulse height distribution measured at a few locations at wire 55 are shown in Fig. 4.4. The distributions correspond

to areas with no, small and large gain loss respectively, as can be seen in fig 4.3. We see that in areas with gain loss, the pulse height distribution becomes broader, and with a lower average value.

Not all current changes are due to aging effects. The atmospheric pressure during the scan, for instance, modifies the gain. A 1% increase in pressure causes about a 5% decrease of the gain. Another problem is that the 20 mCi scanning source is placed above the center of the module, which results in consistently lower currents in wires at the edges of the module. To separate such overall or constant current differences from aging effects, we divide the current measured in the scan made after the irradiation by those measured before the irradiation. The resulting two dimensional 'map' of the gain changes is quite effective for determining aging effects, and is used throughout this report.

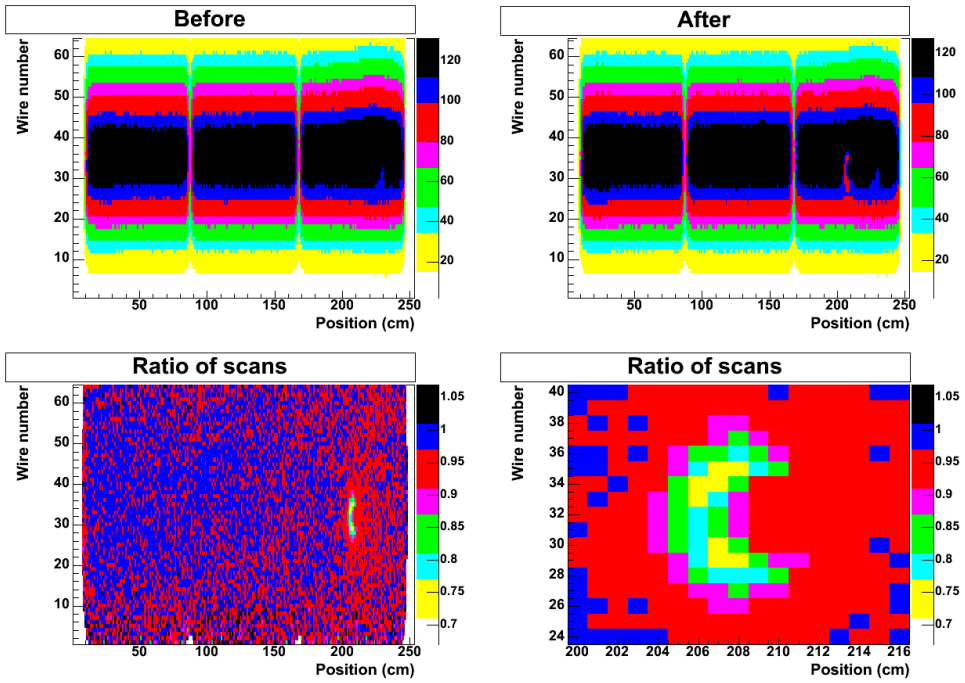

Figure 4.5: *The results of scanning a module before and after an irradiation test with a 2mCi ^{90}Sr source, placed at 208 cm above wire 32. The gas flows from left to right. The results of the scans are shown in the top, where the color scale notes the currents in nA. The lower graphs show the values of the division of the top two graphs. [Module 58, 31/01/2007]*

As an example, Fig. 4.5 shows the results of scanning a module before and after a typical aging test. As described, the module was scanned before and after it was irradiated for 20 hrs with the 2mCi source. This source was placed above wire 32, at 208 cm. The top left and right graph show the currents (on the color scale in nA) measured before and after the irradiation respectively. One can see that the currents near the center wires are considerably higher than at the edges as expected. Furthermore, there are two thin regions with

low currents visible. This is due to wire locators inside the straws at these locations. By comparing the two graphs, one can already see the aging effect. Around 208 cm there is a small area with lower currents after the irradiation.

The lower left graph shows the results of dividing the second scan by the first. The average of the division is not exactly 1, due to air pressure differences. But the resulting map is smoother, without distortions due to the wire locators or the scan source profile. The aging damage is more clearly visible on this ratio plot. On the lower right graph one can see a zoom-in on the aging damage from the previous graph.

A few of the unusual characteristics of our aging phenomenon are immediately apparent from the crescent shape of the damage profile (the area with a significantly lower gain than would be expected) in Fig. 4.5.

- Less gain loss at high intensities at 208 cm.
- More gain loss upstream of the source at positions below 208 cm.

The collimated source used for the irradiation gives the largest intensity right below the source. The crescent shape shows that the area that receives the largest intensity does not necessarily have the largest gain loss. This is in contradiction with the implied assumption of most other experiments that dealt with aging. That assumption shows, for instance, in the common definition of aging in terms of %/(C/cm/wire). But Fig. 4.5 shows that in our case, that definition can be misleading. If the intensity of our source is indeed the highest right below the center, then the area below the center will obtain the most collected charge per cm per wire. But that area does not have the highest gain loss. So the aging in %/(C/cm/wire) depends on the position with respect to the source. Right below the source, the aging is about 10%, with an intensity of about 60 nA/cm/wire, resulting in an aging rate of 2500 %/(C/cm/wire). But at the areas with the highest gain loss, the aging rate is over 70,000 %/(C/cm/wire).

Figure 4.5 also shows that the damage profile is not symmetric, even though the source used for irradiation is. Especially at the central wires, there is much more damage to the left of the source center than to the right. All standard irradiations we performed show this asymmetry. Its direction depends on the direction of the gas flow. In Fig. 4.5, the gas flow went from left to right. Most of the damage is thus located upstream of the source. This behavior is unusual in drift chambers. Most literature on aging of drift chambers either does not mention any asymmetry or reports a higher gain loss downstream of the source. In the latter case, it is attributed to polymers created in the avalanche drifting with the gas flow before condensing on the wire. Note that many experiments monitor the detector performance by measuring the response during irradiation. In this way, only the area of highest intensity is monitored. Since many experiments did not investigate the aging as accurately per position as was done in Fig. 4.5, it is possible that upstream damage has occurred before, but remained undetected.

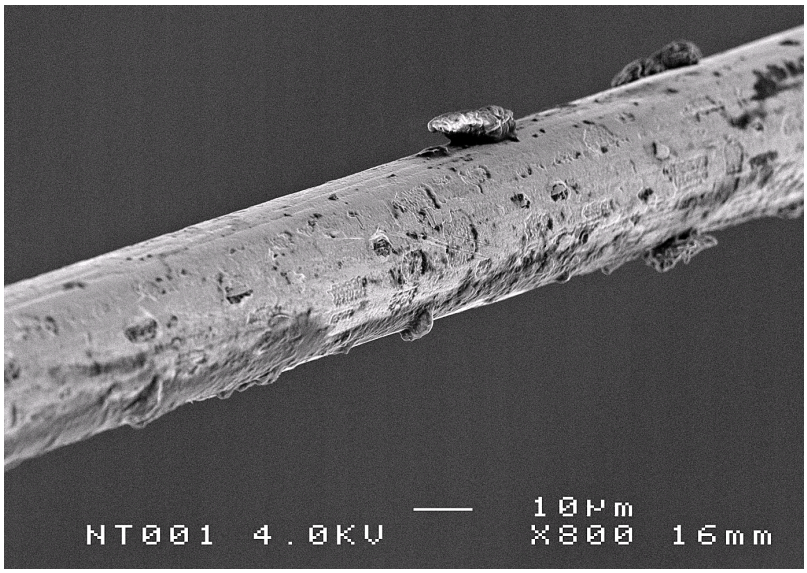

Figure 4.6: *A SEM picture of an LHCb OT wire that showed no aging.*

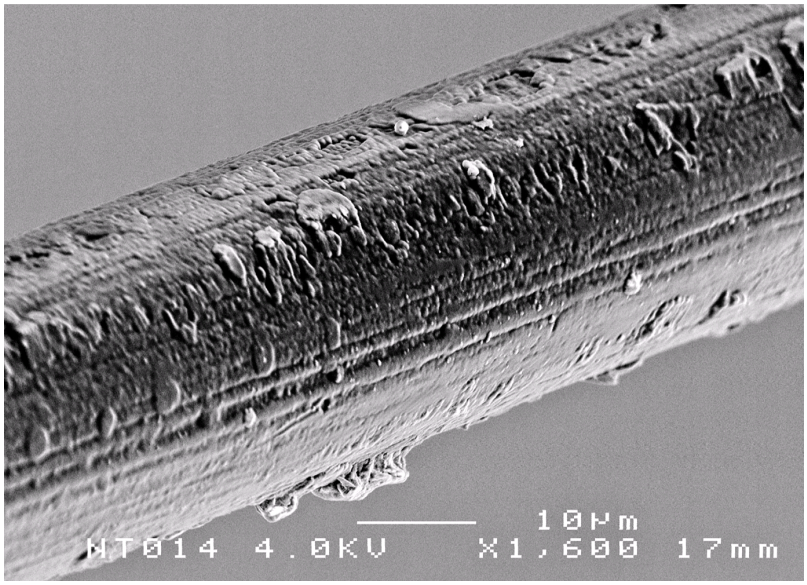

Figure 4.7: *A SEM picture of an LHCb OT wire which showed aging.*

4.2.1 Wire inspection

Our scan method is useful for detecting gain loss, but it does not provide us with information on the cause of the gain loss. To investigate this, several wires have been removed for inspection from the OT modules after irradiations. In Fig. 4.6 and 4.7, images made with an electron microscope from a wire piece are shown with and without gain loss, respectively. The undamaged wire shows a reasonably smooth wire surface, although some small dirt pieces are visible. The aged wire seems to have a lumpy coating over the entire wire surface. This coating appears to be electrically insulating, by the decreasing image quality in the Scanning Electron Microscope (SEM) picture.

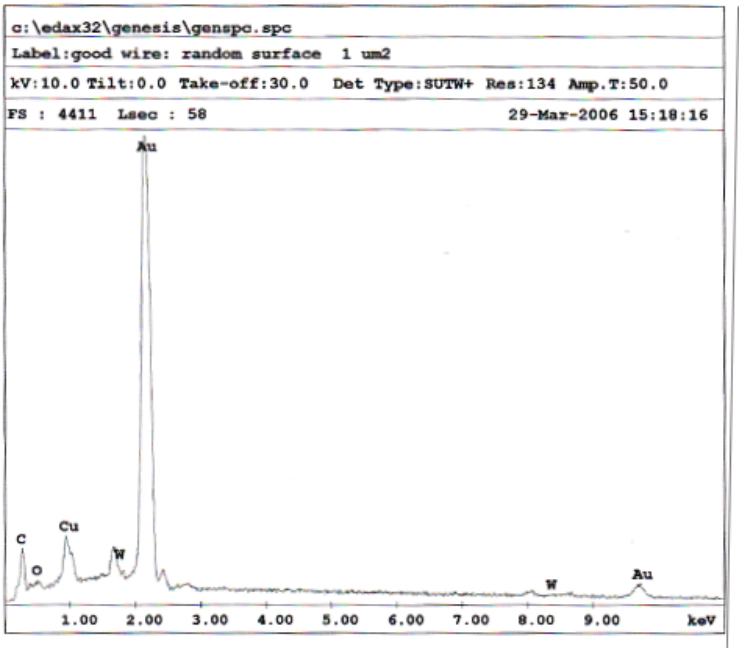

Figure 4.8: *EDX analysis of a normal wire.*

Both wire parts were also analyzed with an Electron Dispersive Spectroscopy (EDX) scan to determine which elements are present in the wire coating. The results are shown in figs 4.8 and 4.9. It is immediately apparent that the aged wire contains a large amount of carbon. Closer inspection reveals a slightly higher oxygen peak. Since we are dealing with insulating carbon deposits, it is likely that hydrogen is present as well, as a part of carbon polymers. However, hydrogen cannot be detected in an EDX scan.

In summary, the LHCb OT modules suffer from rapid gain loss under mild irradiations[1]. This aging appears to be weaker at higher intensities, and mostly occurs upstream of the irradiation source. Inspection of aged wires shows that the gain loss is due to an insulating carbon coating, possibly with slight amounts

[1]No aging effects besides the gain loss, like Malter currents or broken wires, have been observed in the LHCb OT modules with the Ar/CO_2 gas mixture.

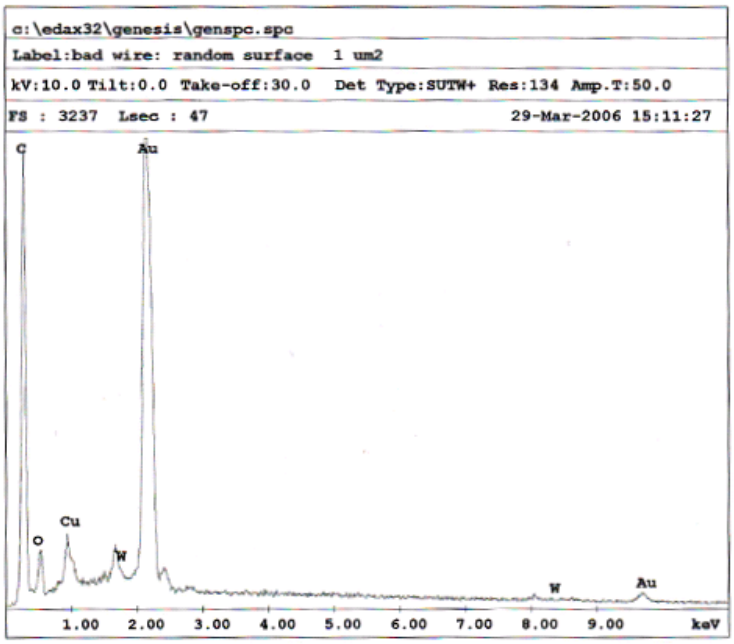

Figure 4.9: *EDX analysis of an aged wire.*

of oxygen.

4.2.2 Quantitative aging measurement

In order to properly investigate the aging rate, we must have a way to quantify the aging. In Fig. 4.5 we showed how the ratio of two scans of a module before and after the irradiation can visualize the gain loss. This ratio plot gives a two dimensional grid of points, each with a different relative gain. We wish to summarize this information in a single value that quantifies the amount of gain loss. Taking the average of the gain in the irradiated area is not the most useful approach, as it is arbitrary which points are part of the damaged area. One could take the average of all points in a large area surrounding the damage, but then the found gain loss is biased because of the large amount of points without damage that are also counted. We therefore need a different description of the aging.

We use two quantitative descriptions:

- The minimum method. We take the average of the two points in the irradiated area which show the highest gain loss, and normalize this to an unirradiated region. This will give a value between 0 and 1. A value of 0 would mean that there is no signal after irradiation, a value of 1 would indicate no gain variation. As an example, analyzing the aging profile in Fig. 4.5 results in a value of 0.74 ± 0.02 (with a bias of approximately -0.03 if the gain loss is negligible).

- The integral description. For each point near the irradiated area, the relative gain is normalized to the relative gain in an unirradiated area. This should give a value of 1 at each point if there are no gain variations. The deviation from 1 is summed for all points. This give a total value of 0 if there are no gain changes in the irradiated area. If there is significant gain loss, the total value will be negative. In the case of Fig. 4.5, a value of -13.4 ± 0.7 is found.

4.3 Aging parameters

Several common features of the observed aging effects were discussed in section 4.2. However, there are also several variations that are observed between irradiations. In this section we will test the effects on the aging in LHCb OT modules by varying several parameters. In sections 4.3.1 and 4.3.2, we show that variations in the intensity and the collected charge during the irradiation have a different effect on the aging rate than expected. The effect of increasing the duration of the irradiation is also discussed in section 4.3.2. Furthermore, we show the results of varying the gas flow, the irradiation location, the high voltage and the source type.

4.3.1 Collected charge and intensity

In most literature on aging effects, the key parameter is the collected charge per centimeter of wire (C/cm). Usually, the aging is presented as a percentage of gain loss per C/cm. This suggest an assumed linear relation between the amount of aging and the collected charge. This neglects the possible dependence on the intensity of the source. In our case, we find that a linear dependence on the intensity breaks down as discussed in section 4.2.

We wish to further study this effect, and describe the gain loss as a function of intensity in nA/wire/cm. Our setup can only determine the integrated current along the entire wire (nA/wire). But the 2mCi source used for (most) irradiations has a spherically symmetric current profile. By fitting the one dimensional data with an appropriate function, we can reconstruct the two dimensional source profile. A two dimensional function that describes the data well is a triple gauss:

$$I(x,y) = A_1 \exp\frac{x^2+y^2}{\sigma_1} + A_2 \exp\frac{x^2+y^2}{\sigma_2} + A_3 \exp\frac{x^2+y^2}{\sigma_3}. \tag{4.1}$$

Here I is the intensity in nA/cm, and x and y are the distances from the center of the source in the direction parallel and perpendicular to the wires, respectively. The position of the source along the wire, x, is measured by hand, whereas the distance to the wire, y, is determined by the fit. To get the function for the one dimensional profile, we must integrate over x, over the length of the wire. Because the wire length is much larger than the width of the Gaussian,

we approximate this by integrating from -∞ to ∞. This gives us

$$F(x,y) = C + \sum_{i=1}^{3} A_i \sqrt{\pi}\sigma_i \exp \frac{y^2}{\sigma_i}, \tag{4.2}$$

where the constant C is added to account for the noise from the current meter.

Figure 4.10 shows the result of analyzing a typical irradiation in this manner. We are currently only considering the area upstream of the irradiation point, since the damage of the aging is located there.

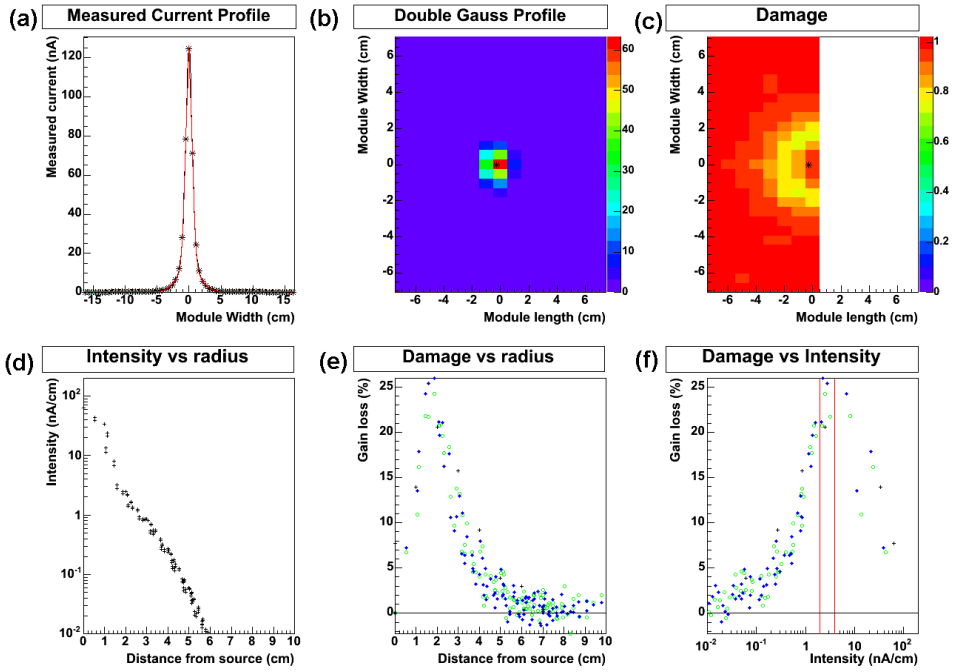

Figure 4.10: *An analysis of a typical 20 hour irradiation with the 2mCi ^{90}Sr source. [Module 58, 31/01/2007]*

Figure (a) in Fig. 4.10 shows the one dimensional source profile (the asterisks) and the fit of the profile with function Eq. 4.2. Figure (b) shows the resulting two dimensional profile, provided by function Eq. 4.1, using the values for the fit parameters from Eq. 4.2. The location of the source is shown by the asterisk. Figure (c) shows the damage profile, based on the scans. Only the half under consideration, upstream of the source, is shown. Figure (d) shows the intensity in nA/cm as a function of the distance from the center of the source. Figure (e) shows the damage in each point from graph (c), as a function of the distance from the source[2]. Figure (f) is a combination of the previous two,

[2]Points coming from wires lower than 32, higher than 32, and wire 32 are shown as hollow circles, diamonds and crosses respectively. The distinction is made to be able to investigate asymmetries in the damage between the left and right half of the module. This is required, for instance, when investigating HV training on one half of the module, see chapter 7.3.

showing the gain loss as a function of the intensity. The two vertical lines at 2 and 4 nA/cm are reference points to guide the eye.

From Fig. 4.10 we can see that damage does not simply increase, let alone linearly increase, with the intensity and therefore the collected charge. Rather, there is a peak in the graph, indicating a particular intensity that causes the most aging damage. This intensity seems to be between 2 and 4 nA/cm.

In order to further investigate the relation between the intensity, the collected charge and the amount of aging, several irradiations with different collimators were done. The different collimators change the intensity measured at each point, although the shape of the profile stays roughly the same. Figure 4.11 show aging profiles for different collimators. The graphs are labeled with the total current measured in the center wire. All irradiations were roughly 20 hours long, so the collected charge is proportional to the intensity for the various irradiations. Figure 4.12 shows plots of the damage as a function of the intensity for the same irradiations.

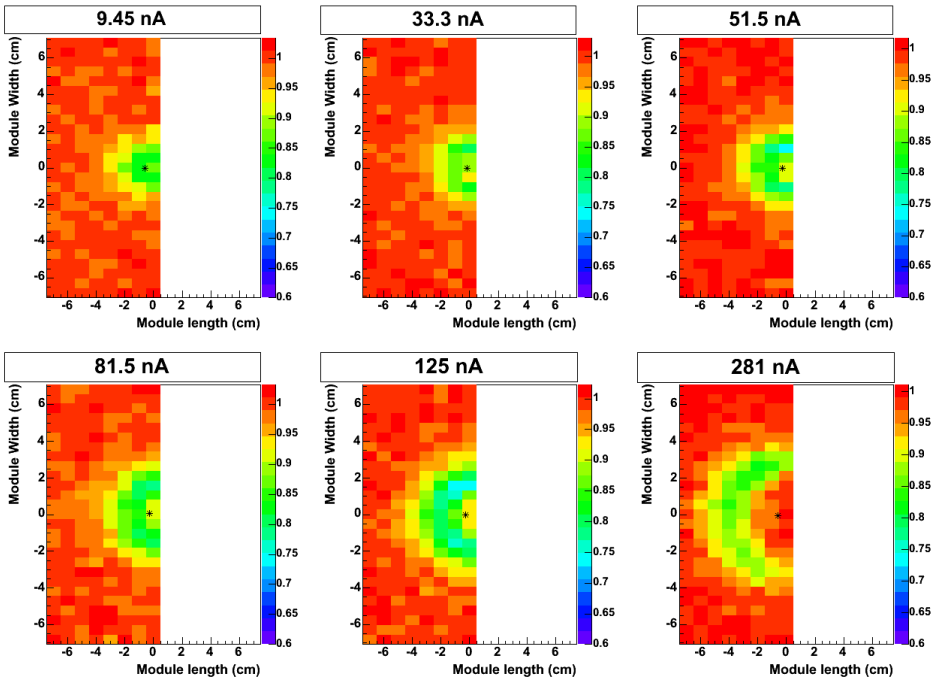

Figure 4.11: *Scans of the aging profiles for different collimators, resulting in different intensities. [Module 58, 31/01/2007-08/02/2007]*

Figure 4.11 shows clearly that the damage does not simply increase with the collected charge or intensity. As the intensity increases, the damage profile broadens, but does not become 'deeper'. And while there is a lot of damage right below the source at low intensities, the damage there actually decreases at higher intensities. At the highest intensity, there is barely any damage near the center of the source.

This picture is confirmed by Fig. 4.12. Even when the range of intensities

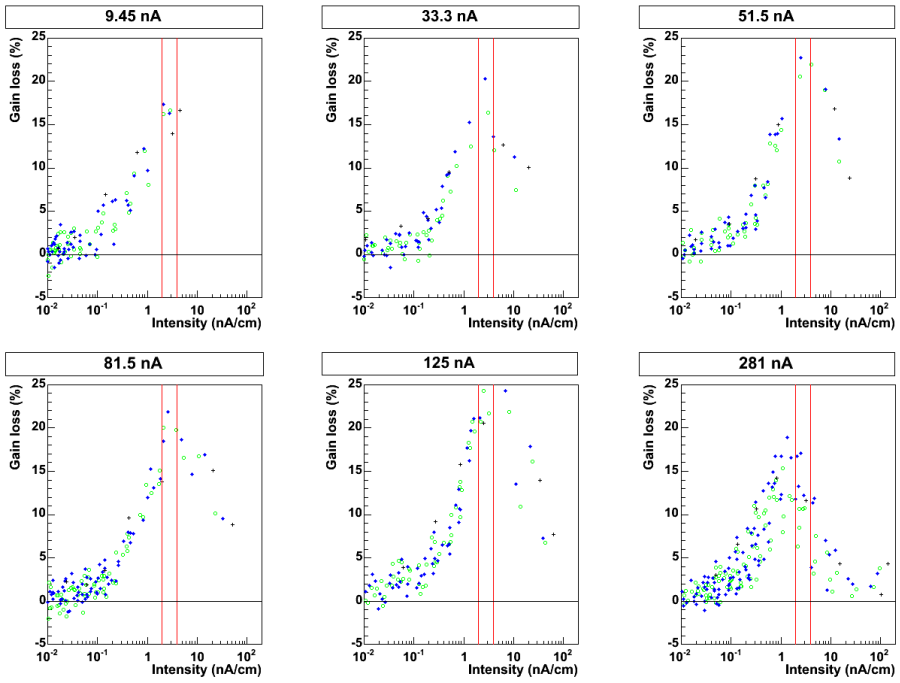

Figure 4.12: *The amount of aging as a function of the distance from the center of the source for different collimators, corresponding to the aging profiles in 4.11.*

under consideration changes, the maximum damage occurs roughly at the same intensity. This suggests that the shape of the damage profile is the result of the dependence of the damage on the intensity or the collected charge.

The cause of this dependence is not well understood. There are three separate models that could account for this behavior:

- Space charge model. The appearance of space charge is the most commonly used explanation for a decreasing aging rate with increasing intensity in literature (see section 5.1). Space charge around the wire is thought to spread out the avalanche over a larger region, thereby reducing the density of radicals that can form polymers. The tests shown in section 4.3.7 found no evidence of space charge in LHCb OT modules. As such, there is no evidence that the space charge model is the correct explanation.

- Depletion model. In this model we assume that the gas mixture contains a small amount of some substance that causes carbon deposits when irradiated. Once the gas reaches the irradiated area, carbon deposits begin to form. The rate of formation does increase with intensity. However, the amount of the substance is limited. Once all of the substance has been used in the formation of carbon deposits, only the inert gas mixture remains behind. In this model we assume that the substance is depleted

before the region at high intensity is reached. This model explains the upstream-downstream asymmetry of the damage profile, and can explain the lower aging rate at lower gas flows, as documented in section 4.3.3[3].

- Balance model. This model assumes that not all radicals formed under irradiation cause deposits. Some can bind with the carbon to form stable gas molecules, which are transported away by the gas flow. These radicals can be created at higher intensities than the products that do cause deposits. In that case, we see no aging at higher intensities because these *beneficial* radicals are also produced. Only at moderate intensities there is sufficient carbon formation without the creation of sufficient radicals. The shape of the aging profile depends on the balance between the creation of the two types of radicals. If the beneficial radicals live long enough, they can also prevent aging downstream of their point of creation. This also explains the upstream-downstream asymmetry. This model also explains the aging effect with no gas flow (where the upstream-downstream asymmetry vanishes, but the intensity dependence remains, see section 4.3.3) better than the depletion model[4].

There are indications for both the depletion and the balance model. With our current data, we cannot conclude which is correct.

4.3.2 Time

Normally, one would expect the dependence of the aging on the irradiation time to be contained in the dependence on the collected charge. But as we saw in section 4.3.1, the aging might not increase linearly with the collected charge, which would also mean that the dependence on time is not what we would expect. Therefore, a test is needed that can discern the effects of intensity and collected charge on the rate of aging.

To determine the effects of increasing collected charge without increasing intensity, one position was irradiated for an extensive period. During the irradiation the intensity remained approximately constant. Figure 4.13 shows the time evolution of the damage of this irradiation. The different scans are labeled by the total amount of irradiation time. The collected charge is proportional to the irradiation time. The corresponding plots of the damage as a function of the intensity are shown in Fig. 4.14. Note that these irradiations took place after a HV training session on the lower half of the module. Therefore only the upper half of the scans in Fig. 4.13, and only the corresponding blue diamonds in Fig. 4.14 should be considered for this analysis. In section 7.3 the effects of HV training will be discussed further.

[3]It can also explain why in cases with very strong aging, the damage profile changes from a half moon to a spherically symmetric profile with a high gain loss at the center of the source. Once the upstream area has suffered sufficient gain loss, the received currents at that location will be lower. This slows the radical formation, and allows the aging substance to reach the area with higher intensities.

[4]The radicals might also react with pollution already on the wire, which would explain the cases where a gain increase directly below the source was detected. Figure 4.18 shows an example of this effect.

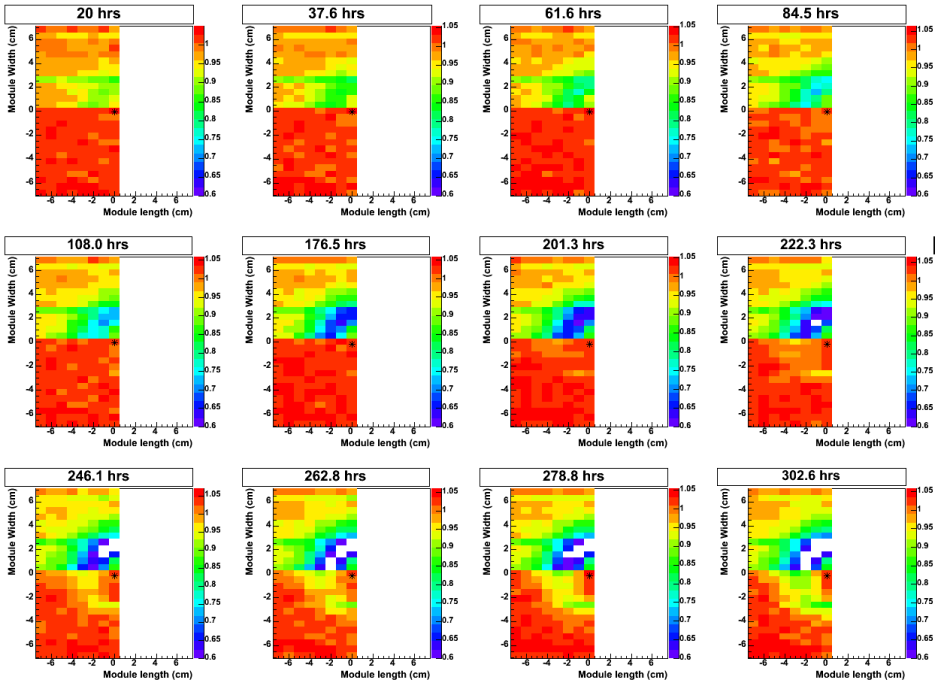

Figure 4.13: *Scans of the aging profiles after different periods of irradiation. The intensity is approximately constant. [Mod 3, 20/08/2006 - 06/09/2006]*

The top left corner of all scans in Fig. 4.13 show the characteristic half moon shape. It is quite clear that as the irradiation time and the collected charge increases, the 'depth' of the aging profile increases, but the shape does not notably change. This is unlike the result observed in Fig. 4.11, where the shape of the profile changed considerably as the collected charge increased. The key difference is that here, the intensity is approximately constant between the different scans. The conclusion must be that the shape of the aging profile depends only on the intensity.

This is confirmed by Fig. 4.14. In all cases the damage as a function of intensity peaks at the same point around 2-4 nA/cm, regardless of the irradiation time. Figure 4.14 also shows that the amount of damage increases monotonously with the irradiation time. However, since the effects of increasing the intensity and the effects of longer irradiation times are not the same, one cannot quantify the aging as a simple function of the collected charge. The collected charge per cm is, after all, the product of intensity and time. Using the collected charge as a variable requires that the effects of changing intensity or time are equivalent. Therefore, time and intensity shall be used as separate parameters, and collected charge will not be used.

Finally, Fig. 4.15 visualizes the progression of the amount of aging as a function of time. The minimum method and integral method, as described in section 4.2.2, are used to quantify the amount of aging[5]. We see that the

[5]The area around the source used in the integration method is smaller than usual, since we

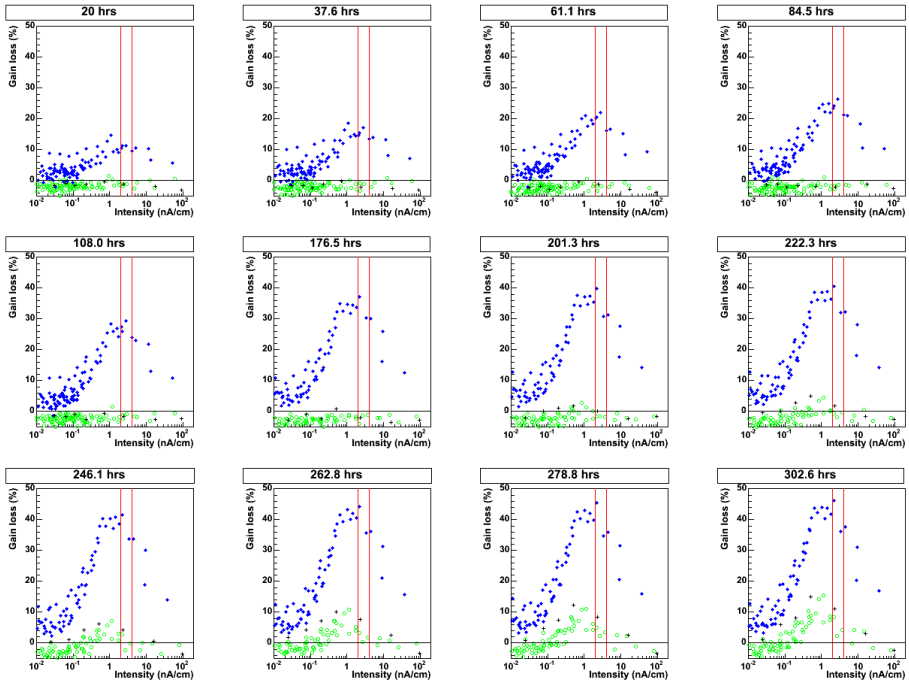

Figure 4.14: *The amount of aging as a function of the distance from the center of the source after different periods of irradiation, corresponding to the aging profiles in 4.13.*

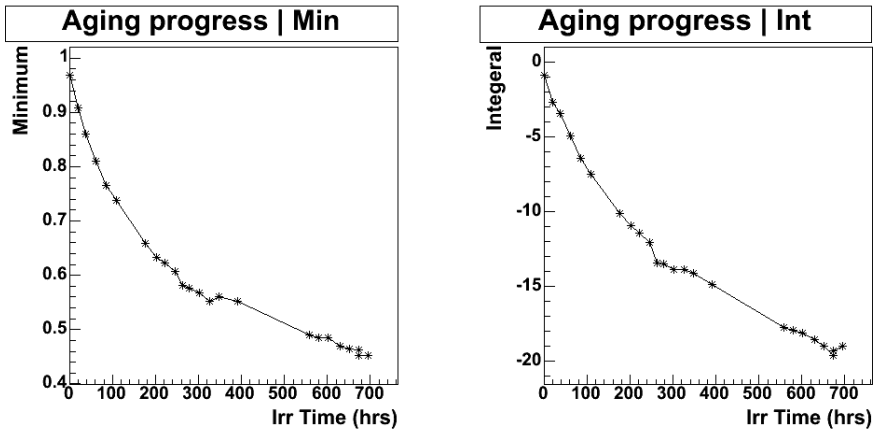

Figure 4.15: *The amount of aging, measured with the minimum and the integral method, as a function of irradiation time.*

progress is approximately linear for short times, although the slope seems to flatten of as time increases. This would be expected, since the the aging cannot continue to increase once 100 % of the gain is lost. But for moderate amounts of gain loss, the linear approximation remains valid.

We find that the aging rate, and with it the slope of fig 4.15, varies strongly between modules. Even modules that have a similar production and treatment history may show strongly varying aging rates. As mentioned before, this is a probable indication of hidden parameters. The rate of aging should be determined separately for each module.

4.3.3 Gas flow

As mentioned before, the characteristic crescent aging pattern is always oriented the same with respect to the gas flow. The asymmetric gap is always downstream of the irradiation point. This suggests a dependence of the aging effects on the gas flow.

One of the effects the gas flow has is changing the rate of aging. The gas flow in the final LHCb setup will be 10 l/hr. Since early 2006, aging tests have been performed with a gas flow of 20 l/hr. This was done because a higher gas flow seemed to cause quicker aging, meaning our aging tests could be performed faster.

The results of aging tests performed with various gas flows are summarized in Fig. 4.16. The ratio plots seem to confirm that a slower gas flow results in a slower aging rate. The irradiation done with no gas flow shows an especially interesting effect. In the absence of a gas flow, the aging profile no longer has a preferential direction. Instead of a crescent shape, the aging profile appears to be more of a donut shape[6]. The area without gain loss in the center does show that the previously mentioned intensity effect remains even when there is no gas flow (which agrees with the balance model, see section 4.3.1)[7].

The last graph in Fig. 4.16 shows the aging measured with the minimum method in all tests with lower gas flows. They are all compared with a standard irradiation done at 20 l/hr, performed on the same module in the same time period (shown in the legend). This eliminates the difference in aging rates due to module characteristics, flush time, etc. This graph confirms that higher gas flows cause more aging.

4.3.4 Position

It is possible that the rate of aging depends on the location of the irradiation point. Tests have been performed to test this possibility. Figure 4.17 shows the aging, measured with both the minimum and integral method. In the left graphs, the aging is shown as a function of the distance between the gas input and the irradiation point. Although there are variations in the aging rate, they

only care about the aging in the wires above 33. The other wires have received HV training.

[6]Because the straws are 0.525 cm, and the illuminated area is 2 cm wide, the shape is not perfectly circular.

[7]There seems to be a rectangular are of lower gains around the irradiated area. This is not due to aging, but to pieces of tape placed on the module to denote the irradiated area.

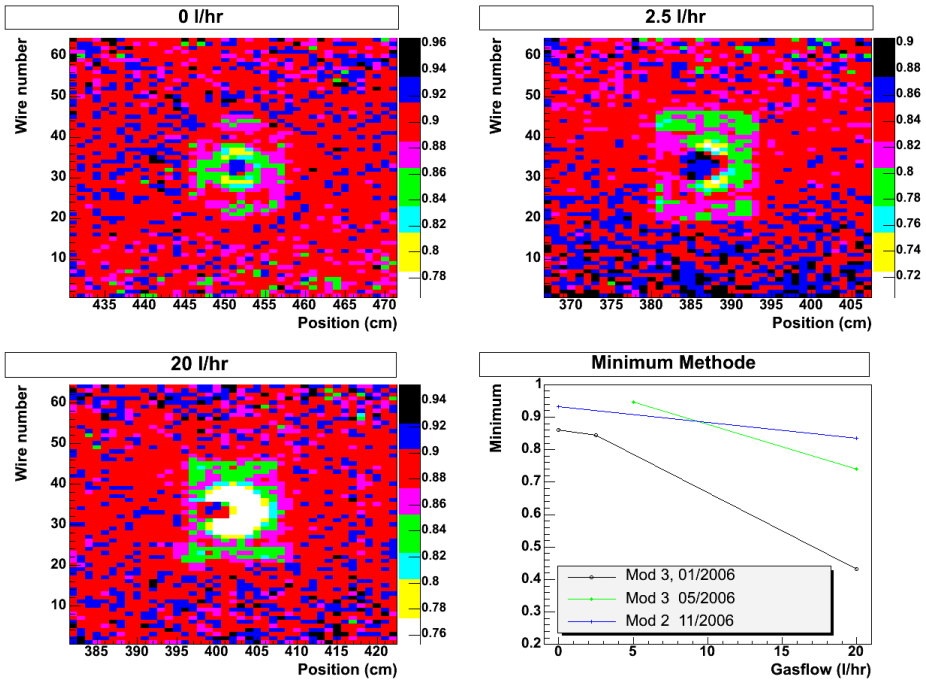

Figure 4.16: *The effects of different gas flows on the aging. The first 3 pictures show scans done after irradiations at different gas flows. The last graph shows the amount of aging (measured with the minimum method) as a function of the gas flow measured at different times and modules.*

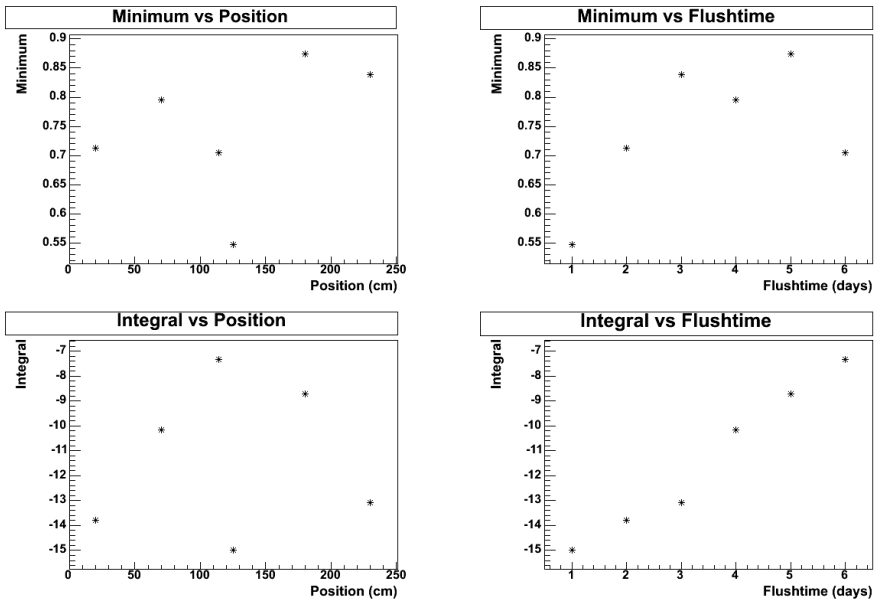

Figure 4.17: *Aging as a function of position and flush time, measured with the minimum and integral method. The values are corrected for small differences in irradiation time. [Module 3, 13/04/2006 - 18/04/2006]*

do not appear to depend on the position of the irradiation point. The right two graphs in fig 4.17 show that it is more likely that the variations depend on the time that the module was connected to the gas flow. On average, the aging rate decreases with an increasing flush time[8]. More data on this effects is shown in section 7.1. No dependence on the position has been found in a standard F module.

4.3.5 Voltage

The effect of the voltage on the aging rate has also been tested. A well known effect of lowering the voltage is that the gas gain is also lowered, resulting in lower currents. In section 4.3.1, the effects of lower currents on the aging has already been discussed. In order to only see the effect of a different applied voltage, different collimators were used. The collimators were chosen such that the source profile was comparable at the different voltages.

The divided scans of irradiations at a low, normal and high voltage are shown in Fig. 4.18. Although some variations in the aging profiles are visible, they appear to be comparable. The values found with the minimum method for these three irradiations are 0.653, 0.692 and 0.658 respectively. The integral method finds -13.33,-12.97 and -16.00 respectively. These values indeed correspond to comparable aging rates. We conclude that the voltage has no significant effect on the aging rate beyond the effects of the changed intensity.

[8]Flushing time should not be confused with irradiation time as shown in Fig. 4.15

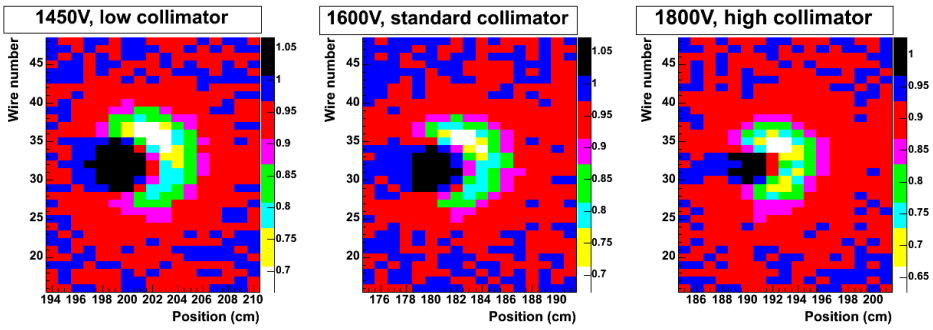

Figure 4.18: *Aging measured at various voltages. The different collimators provided comparable source profiles. The chronological order of these irradiations was: 1600V, 1800V, 1450V.[Module 3, 17/04/2006 - 27/04/2006]*

4.3.6 Radiation

Most of our irradiation tests are performed with a ^{90}Sr β source with energies of up to 2 MeV. But within the LHCb environment the modules will be irradiated with a mixture of photons, leptons and hadrons. It is possible that certain passing particles cause different aging effects than others. Unfortunately, there are only a few types of radiation that we can provide in our setup. Aside from β radiation, we can use a ^{55}Fe γ source with 5.9 KeV. Aside from these two sources there were previous tests, performed elsewhere, with hadronic radiation (See section 4.1). Those tests detected no aging, but were performed at higher intensities and with a different gas mixture.

Figure 4.19 shows the ratio plots after irradiations with a ^{90}Sr and a ^{55}Fe source. The upper two irradiations were performed at a different time than the lower two. Both pairs can therefore only be compared with each other. For both the upper and the lower graphs, it is apparent that an irradiation with the ^{55}Fe source causes less aging. However, one cannot conclude that this is due to a difference between β and γ radiation. The ^{55}Fe source gives a lower but broader current profile, which could be the cause of the deviations. It is important to note that the characteristics of the aging profile remain the same. In all cases, the gain loss is concentrated in a semi circle upstream of the irradiation point.

Figure 4.20 shows the damage as a function of the intensity for the same irradiations. The spread of the damage appears to be larger than in Fig. 4.12. This is due to the uncertainty of the source position for these irradiations. The strongest damage appears to be caused at roughly the same intensity for the different sources. In the upper case, the peak is around 1 nA, in the lower case around 0.5 nA. The total amount of gain loss is lower with the ^{55}Fe source, but this was found to happen at lower intensities with the ^{90}Sr source as well. We therefore conclude that the aging effects of β and γ radiations do not differ significantly.

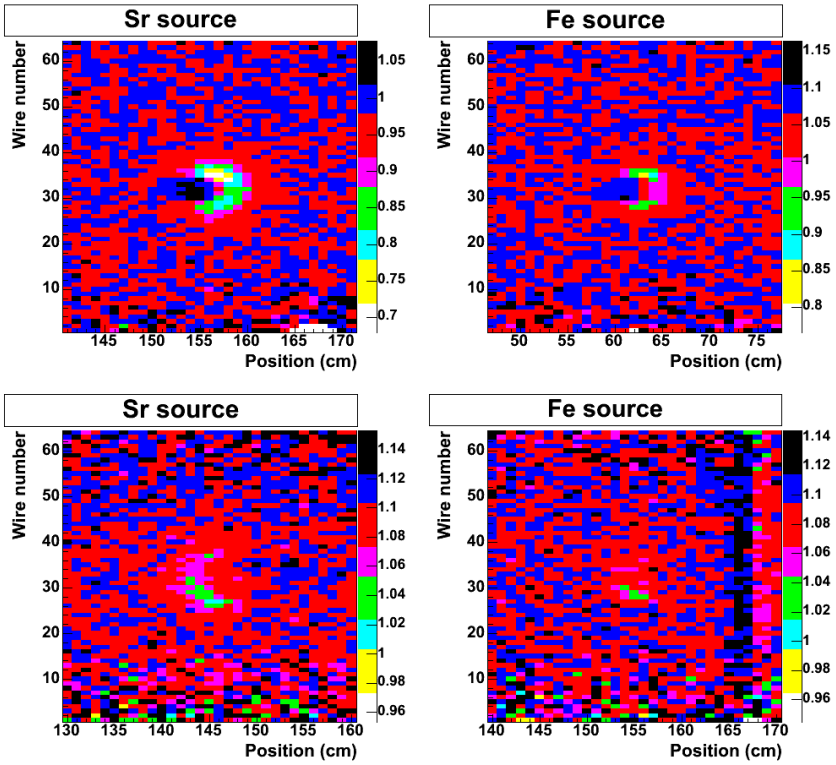

Figure 4.19: *Comparison of the aging caused by a ^{90}Sr and a ^{55}Fe source. Note that in the lower two graphs, the scale is different than in the upper graphs. [Module 3, top: 05/06/2006, bottom: 20/11/2006]*

4.3.7 Space charge

Previous experiments that observed lower aging at higher intensities often contributed this to the appearance of space charge (See section 5.1). Space charge is said to arise at high irradiation densities. Particles pass at such a high rate that the electrons and ions of an avalanche have not yet dissipated when the next particles passes through and causes an avalanche. The charged particles that are still around the wire modify the electric field, which influences further avalanche creation. In effect, space charge can lower the gas gain. Although it is not a parameter that can be independently varied, it is relevant to study whether or not it appears under normal operating conditions.

In order to test if space charge is created in common aging tests of the LHCb OT modules, we have performed a brief irradiation at various operating voltages. The gas gain, and with it the measured currents, increase exponentially with the voltage in the absence of space charge. Figure 4.21 shows a schematic view of our space charge test. When the operating voltage is low (a), no space charge occurs and the measured current in each wire is proportional to the amount of irradiation. A higher operating voltage will increase the overall gas gain (b). If space charge is created at higher intensities, it will lower the

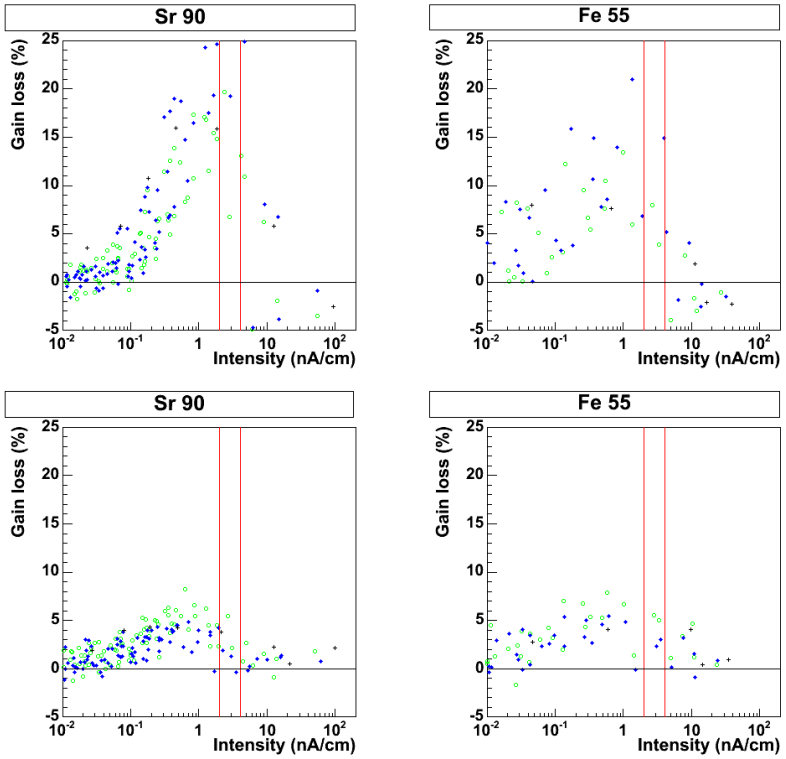

Figure 4.20: *Damage as a function of the intensity, based on the graphs in fig 4.19.*

gas gain and thus the measured currents at high irradiation intensities. The measured currents at lower intensities will not be affected. To check for space charge effects, the current profiles at low and high voltages are scaled to compare them (c). If there are space charge effects, the peak of the profile at a high voltage will be low relative to the peak at a low voltage. Alternatively, we can scale both graphs by setting the peak intensity equal (d). Since space charge would lower this peak at higher voltages, this should result in a broader profile compared with the profile of a low voltage. If there is no space charge at either voltage, the profiles should have the same shape.

Figure 4.22 shows the resulting current profiles. The graphs show the currents measured at each voltage. Figure 4.23 shows the scaled current profiles measured at each. All profiles appear to be the same. The profiles measured at higher voltages do not appear to cause relatively lower currents at the peak of the profile. In fact, the last graph shows that at *lower* voltages the profile is broader, with higher relative currents away from the peak of the irradiation. This is opposite to what could be expected from space charge effects. The effect is due to the low absolute currents in this region. As can be seen from the first graph, many of the wires measure less than 1 nA, which is close to the sensitivity of our setup.

We conclude that at the normal operating voltage of 1600V and at rea-

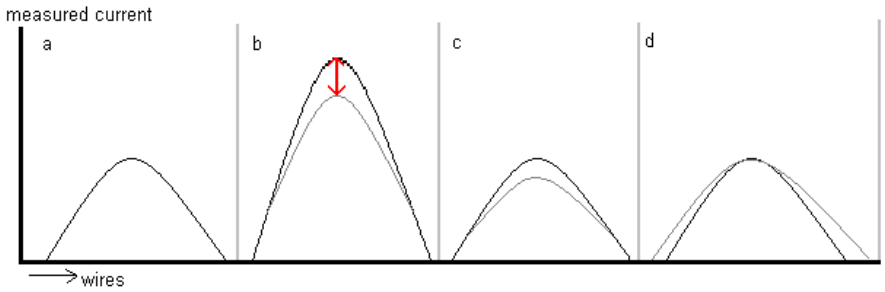

Figure 4.21: *An example of the effects of space charge. (a) The currents measured at a low voltage, without space charge. (b) The currents measured at a high voltage, with space charge that causes lower currents than would be expected from simply scaling the profile in (a). (c) The profile of a low voltage compared with the profile at a high voltage, scaled to eliminate the effect of the voltage. The high voltage case will show lower currents, due to space charge effects. (d) The profile of (a) compared with (b) scaled such that the maximum currents of the profiles match. This raises the tails of profile (b), since those are not affected by space charge.*

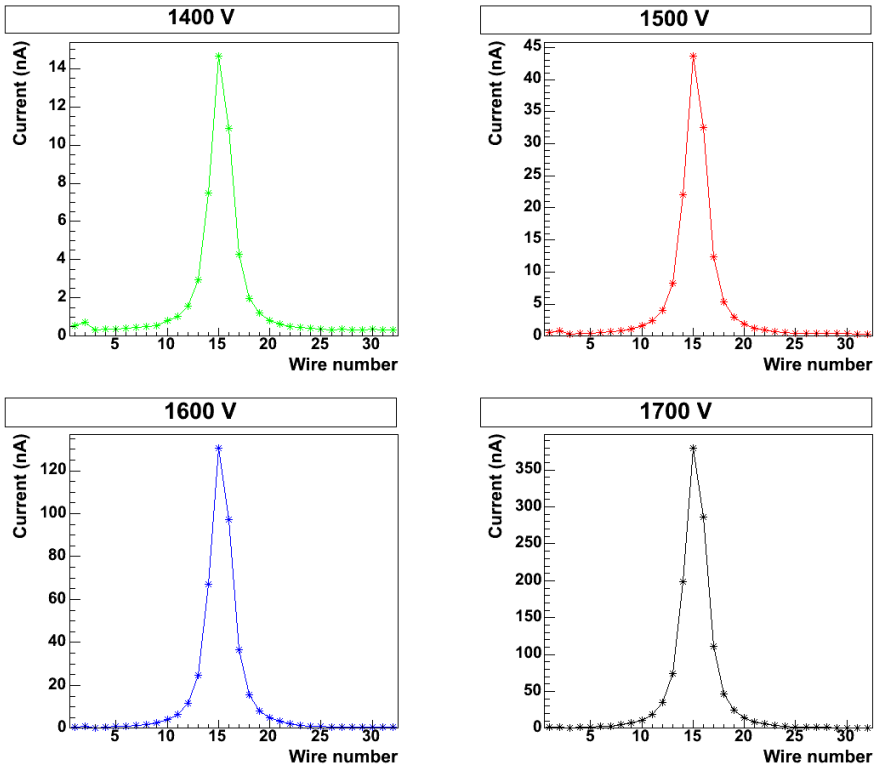

Figure 4.22: *The current profile of a ^{90}Sr source, measured at various voltages. [Module 121, 13/08/2007]*

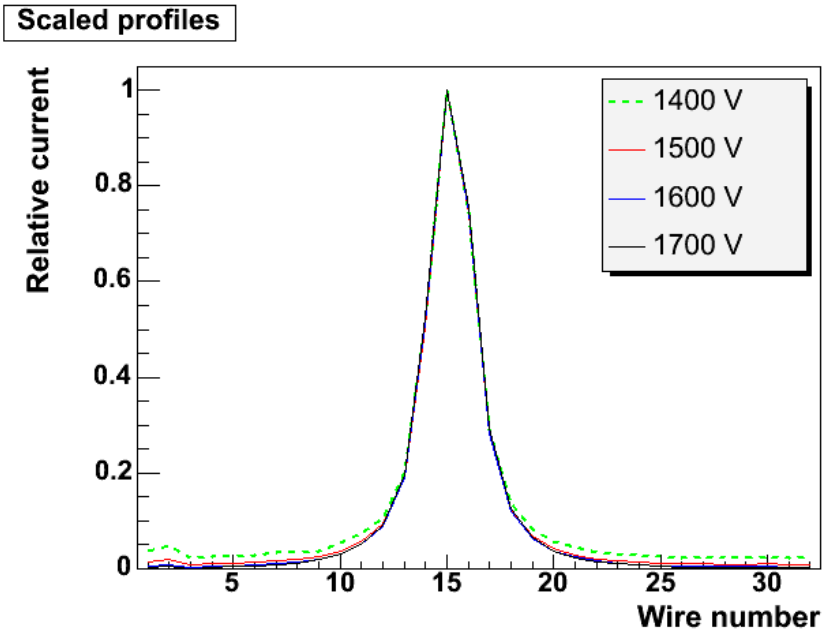

Figure 4.23: *The relative current profiles, scaled to a maximum of 1. The curves for 1500-1700 V overlap almost completely. The tails of 1400 V are slightly higher.*

sonable irradiation densities, there are no significant space charge effects in the LHCb OT modules. The lower aging rates at higher intensities cannot be attributed to space charge.

4.4 Summary

The aging seen in the LHCb OT modules has several distinctive features, such as the low aging rate below a small source and the high aging rate upstream of the irradiation. Our scanning method allows us to study these characteristics. To give a quantitative estimate of the aging, two separate methods have been developed.

The aging effects in their current form were first observed in 2005. Aging tests done prior to that time indicated that our the LHCb OT would not show aging effects with the present module design and gas mixture. It is unclear why no aging was seen in earlier tests. The most plausible assumption is that those experiments were performed at much higher intensities than the current tests and that the region upstream of the source was not investigated in detail. In addition, these older aging tests were all done with prototype modules.

The effects of several parameters on the aging have been tested. It has been shown that the collected charge is not a useful parameter, even though it is the main parameter in most aging experiments. Increasing the intensity or the irradiation time seems to have different effects, while a simple dependence

on the collected charge indicates that the two should be equivalent. However, we have found that only increasing the irradiation time increases the gain loss. Increasing the intensity, on the other hand, mainly changes the area where the highest gain loss is found.

Furthermore, we have found that the gas flow also affects the aging. The gain loss is concentrated upstream of the source. When the gas flow is turned off the aging profile appears to be symmetrical. At low, but non-zero gas flows, the gain loss of an irradiation is lower than at high gas flows.

Several other potential parameters were also investigated. The aging rate does not depend on the irradiation position, although it does depend on flushing time (See section 7.1 for more details). The voltage applied to the wire, and the irradiation source type used, also seem to have no effects on the aging beyond the known intensity effects. No evidence for the appearance of space charge has been found.

Chapter 5

Previous experiments

In this chapter we will try to give an overview of previous tests on the aging properties of drift chambers. Since the advent of proportional counters and drift chambers, there have been experiments to test their aging properties. This provides us with a large amount of literature on the subject. But of course, not all of the results found in such tests can be applied to our case. We will limit ourself to a few experiments with drift chambers that have similar properties to the LHCb OT, and detectors that experienced the same type of aging effects.

5.1 Intensity dependence tests

As mentioned before, most other aging tests imply that the aging effect scales linearly with the accumulated charge, independent of the intensity. Some reports on accelerated aging tests, which are preformed at much higher intensities than are expected in the actual experiment, note that further tests with lower intensities should be performed. There are few documented cases where a lower aging rate was actually measured at a higher intensity, like we reported in chapter 4.

Most reports that do report such an intensity dependence postulate that this is due to space charge effects. Kadyk proposes [17] that the space charge causes the avalanche to be spread out over a larger region. This means a decreased density of radicals produced in the avalanche, since the volume is now larger. The polymerization rate decreases with a decreasing density of radicals that can form polymers, and so this will decrease the amount of polymer deposits.

For instance, an experiment on the validity of accelerated aging tests for the ATLAS TRT [30, 31] revealed cases where the gain loss was weaker in the center of the source. Figure 5.1 shows the gain loss in each wire as a function of the distance from the center of the source. At 3.6 C/cm, there is almost no gain loss near the center of the source, but significant gain loss at the edges. This is similar to the aging effects seen in the LHCb Outer Tracker, where the aging near the center of the source becomes weaker. Eventually the damage profile becomes 'normal', with the largest gain loss at the highest intensity, at a collected charge of 6.8 C/cm as can be seen in Fig. 5.1 .

These tests were preformed with carbon doped Kapton straws and gold

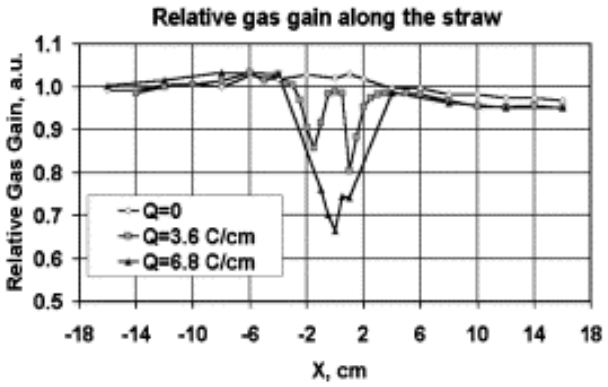

Figure 5.1: *The aging seen in an ATLAS TRT test as a function of the wire position, and thus distance from the source.*

plated tungsten wires, similar to LHCb OT straws. On the other hand, the gas mixture used was a 70/10/20 $Xe/CO_2/CF_4$ mixture. It is not known whether most damage was located upstream, as is the case in the LHCb OT. Nor is it known if the gain loss is due to carbon deposits, or due to some other mechanism. The irradiation doses quoted are several orders of magnitude larger than the doses in a typical aging test done with LHCb OT modules to produce the half moon shaped damage profile. Although it is not specifically mentioned in [30], one can derive an intensity around 350 nA/cm at the area that shows gain loss. According to our derivation in section 4.3.1, that would be two orders of magnitude larger than the intensity at which the LHCb OT experiences the most aging. We cannot confirm that the aging effects seen here are the same as seen in the LHCb OT.

Other cases where lower gain loss at higher intensities was found and attributed to space charge are summarized in [15]. On the basis of a phenomenological model they predict that laboratory experiments will indeed find a lower gain loss at higher intensities, see Fig. 5.2. The upper line is the predicted aging rate in the region of expected LHC conditions for the ATLAS TRT. However, these predictions do not differ from the laboratory predictions below 5 nA/cm. Since the LHCb OT is not expected to receive current densities above 6 nA/cm, the difference between the models is no relevant to us. The graph is presented in [15], but the context and assumptions used to create the graph are not known.

A second explanation for reduced damage at larger intensities is given in [17]. At high intensities, the higher temperature around the wire makes it harder for the polymers to condensate. This is also a possibility in the case of the LHCb OT. But it does not explain why most of the damage is located upstream of the source. The simple model from [17] would rather predict damage downstream, since the created polymers can condensate once the gas flow transports them to the cooler region away from the source.

In summary, there is some precedent on the appearance of stronger aging at lower intensities. However, documentation on this subject is rather scarce, and

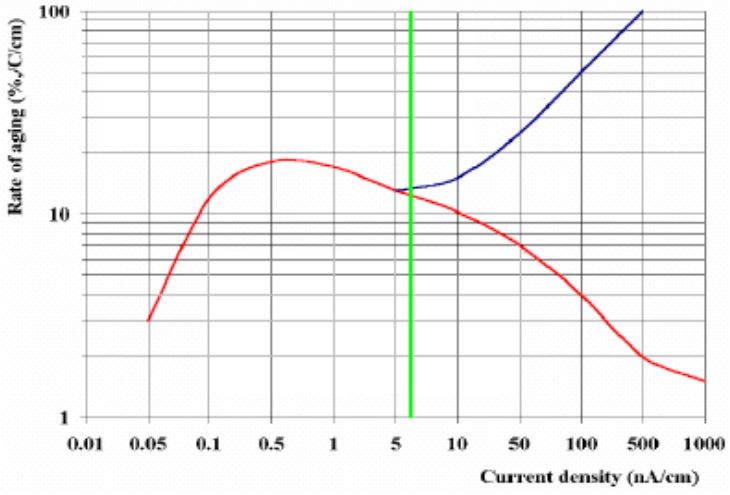

Figure 5.2: *The predicted aging rate as a function of the current density. Created by F. Sauli, its context is unavailable. The added vertical line marks the maximum intensity expected in the LHCb OT.*

thorough reports on the effect and its causes even more so. Most of the reports on this subject suggest that the effect is due to the appearance of space charge. However, an investigation on space charge effects in the LHCb OT, given in chapter 4, does not support this hypothesis in our case.

5.2 HERA-B Outer Tracker

The large hadronic particle flux at the HERA-B [19, 21] experiment provided an opportunity to test detector material and setups in an environment comparable with the LHC environment. The HERA-B Outer Tracker does not use the same straw tube geometry for the cathodes. Instead, a hexagonal honeycomb structure is used to stack two layers of cathode cells on top of each other. The cathode is made of Pokalon-C foil. The anode wires are made of gold plated tungsten.

The various tests with done with the HERA-B OT were not all performed with the same gas mixture. Gas mixtures used include CF_4/CH_4, $Ar/CF_4/CH_4$ and $Ar/CF_4/CO_2$. A rapid gain loss caused by anode aging was seen when $Ar/CF_4/CH_4$ was used. A gain loss of 50 % after a collected charge of 5 mC/cm was observed. Using $Ar/CF_4/CO_2$ did not only prevent this effect, but could actually repair the anode damage done if the chamber was irradiated with $Ar/CF_4/CH_4$ before.

There was one aging effect that occurred in all gas mixtures. The prototype modules proved to be very vulnerable to the Malter effect. Under normal HERA-B conditions, a collected charge of 5-10 mC/cm/wire with a CF_4/CH_4 mixture was enough to produce dark currents, which continued even after the irradiation was stopped. In contrast, a previous test with the same gas mix-

ture but with an external X-ray source, showed no Malter currents up to an accumulated charge of 4.5 C/cm. Further tests proved that only hadronic irradiation could cause the Malter type aging. X-rays and β sources could not cause the Malter effect to occur in clean modules, though they could start the dark currents in modules that already suffered from the Malter effect.

The problem was solved by coating the Pokalon-C cathode film with a 40 nm Au layer on top of a 50 nm Cu layer. Test showed that any kind of coating on the cathode prevented the Malter effect. These new detector cells proved to be fairly aging resistant.

5.3 ATLAS Transition Radiation Tracker

The tests done for the ATLAS Transition Radiation Tracker [32] are relevant to us for several reasons. First, they have reported intensity dependent irradiation damage (see section 5.1). Secondly, the TRT is equipped with similar cathode straws made of Kapton-aluminum and it operates with a $Xe/CO_2/O_2$ (70/27/3) mixture [33]. Finally, the ATLAS TRT tested various detector materials specifically the glue. These tests were the deciding factor when the glue for the LHCb OT was chosen.

These tests with various kinds of glue are summarized in [34]. Among the glues that were tested was Araldite AW103. Irradiation tests indicated that Araldite AW103 caused no aging effects, and did not suffer from outgassing effects. Outgassing refers to the evaporation of a small amount of molecules in the glue at room temperature. These molecules could pollute the gas mixture, and cause deposits.

Because of the positive results with this glue, it was also tested for use in the LHCb OT. Since these tests [26] did not reveal any problems, Araldite AW103 was finally chosen for use in the LHCb OT.

5.4 COMPASS Large Area Tracker

The Large Area Tracker of the COMPASS experiment [35] uses straws with the same composition as the LHCb Outer Tracker [36]. Their straws consist of an inner layer of 40 μm Kapton XC and an outer layer of 12 μm aluminumized Kapton, with a 7 μm glue film in between, but with a 6 mm diameter, as opposed to the 4.9 mm diameter for the LHCb OT.

The radiation hardness of the COMPASS straws has been tested by exposing single straws to a 26 MeV proton beam. Two gas mixtures were used, Ar/CH_4 (90/10) and $Ar/CO_2/CF_4$ (74/6/20). The straw flushed with Ar/CH_4 showed a relative gain loss of 23% after a dose of 1.1 C/cm. Malter currents were observed as well. In contrast, the $Ar/CO_2/CF_4$ mixture showed no significant aging after 1.1 C/cm (<1% gain loss), and no Malter currents. There is no report of broken or etched wires, like the LHCb OT experienced in an $Ar/CO_2/CF_4$ mixture. However, they did observe a 0.1 μm thick deposit on the wire, containing C, N and Si elements. The extra 0.1 μm thickness on a 30 μm wire is not expected

to cause a gain loss larger than 1% if it is electrically conductive, consistent with their results.

5.5 CDF Central Outer Tracker

The CDF Central Outer Tracer (COT) [37] was found to suffer from aging effects that were quite similar to the effects that the LHCb Outer Tracker experienced [18]. Specifically, they found evidence of carbon polymer contamination on the wires of their wire chamber. They also report a dependence on the intensity per cm, not just on the collected charge per cm. On the other hand, they used a different gas mixture, containing ethane instead of carbon dioxide. They suspected that the ethane was the cause of the aging, and their report specifically mentions that carbon dioxide would probably not cause this type of aging.

Another difference is that the COT does not use straw tube cells. Instead, the wires are organized in jet cells that contain 12 wires each. The wires themselves are 40μm and are made of gold plated tungsten. The cathodes are made of mylar foils with vapor-deposited gold.

The CDF experiment performed two runs. The chamber used in run 1 (CTC) was found to have been severely affected by aging at the end of the run [38]. Tests showed a gain loss of up to 100.000 %/(C/cm), comparable with the maximum of 70.000 %/(C/cm) in the LHCb OT. The anode wires were covered with deposits containing mostly carbon, with smaller amounts of oxygen, sodium and silicon. These aging effects could be prevented by flowing the gas through an alcohol bubbler and two different filters. This was an indication that the aging was caused by a polluted gas mixture.

For run 2, the COT was equipped with the filters and bubbler that had been found to prevent the aging seen in run 1. However, a new aging problem was detected after the detector had been operational for more than one year. The definite proof of aging was found by offline tracking in November-December 2003. It was found that the gain on the wires had decreased by 50 % after collecting 35 mC/cm, or 1.400 %/(C/cm). The gain loss was larger for layers closer to the interaction point, and it was also larger near the gas exhaust. This last dependence indicates that polymers are slowly formed in the gas under radiation. Because the polymers drift some time before becoming large enough to form a coating on the wire, there is more aging downstream with respect to the gas flow.

Images of new and aged wires were made using a Scanning Electron Microscope (SEM). Two of these images were shown in Fig. 3.1. The new wires showed a smooth, bright surface. Aged wires showed a dark surface with submicron nodules on its surface. An Electron Dispersive Spectroscopy (EDX) analysis showed, aside from the expected gold peak, a large carbon peak and a smaller oxygen peak. Furthermore, an XPS scan showed that most molecular bonds were either CC or CH, with a small number of CO bonds also present.

The hypothesis of the CDF group was that the ethane quencher was split under influence of either the radiation or the avalanche near the wire. The

resulting CH_2 groups would then start to form polymers. One of the solutions they suggest, based on this hypothesis, is to change the gas mixture to Ar/CO_2[1]. No definite conclusions can be drawn from this however, since the CDF group did not actually prove their hypothesis.

The solution used by CDF is the addition of oxygen to the gas mixture. They had already found that other experiments could reduce aging effects by adding molecules that contain oxygen (such as water). However, when oxygen was leaked into the gas mixture by accident, they immediately noticed a gain increase. The addition of 100 ppm oxygen was able to revert the aging damage of two years in less than two weeks, while further aging was prevented.

5.6 CMS Muon Chamber

Before the production of the CMS Endcap Muon Chambers [39], tests have been done with prototype chambers with several gas mixture including an Ar/CO_2 mixture [24]. They found that operating with the Ar/CO_2 mixture caused aging effects at the anode wire, like with the LHCb OT[2].

The CMS Muon Chambers consist of cathode strip chambers, made of trapezoidal cathode panels. It does not use straw tube cathodes. Instead, there are a large number of wires, running parallel in the same gas volume. Cathode panels are placed on both sides of the wire planes. On one end the cathode is continuous, on the other end it is divided into strips, perpendicular to the wires. By reading out both the wires and the cathode strips, one can determine the location of the passing particle in two dimensions.

The wires used are 50 μm gold plated tungsten, the cathode panels are made of copper-clad FR-4 skins. A prototype chamber was tested with a 30/70 Ar/CO_2 and both a 30/50/20 and a 40/50/10 $Ar/CO_2/CF_4$ mixture.

Tests with the 30/50/20 $Ar/CO_2/CF_4$ showed no anode aging after 13.6 C/cm and a slight increase in the dark currents due to cathode deposits. The 30/70 Ar/CO_2 mixture on the other hand resulted in a 50 % gain drop after every 0.25 C/cm of collected charge. Analysis of the anode wire showed a large amount of deposits. A SEM picture was shown earlier at the right side of Fig. 3.3. The composition of an aged wire showed a large amount of silicon, and sizable amounts of carbon and oxygen.

These results were not unexpected, as the module had been sealed with a relatively simple glue which contained silicon. The CF_4 containing gas mixture was expected to be able to deal with this silicon containment much better. After a refinement of the glue and its contact with the gas volume, the 40/50/10 $Ar/CO_2/CF_4$ mixture turned out to prevent aging as well. Thus the aging problem was solved by using a CF_4 containing mixture, as was originally planned.

[1] Although this is a logical suggestion, based on their hypothesis on the origin of the carbon polymers, it is peculiar that the LHCb OT suffers rather similar aging problems even though it already operates with an Ar/CO_2 gas mixture.

[2] Most other experiments that used a pure Ar/CO_2 mixture did not find such aging effects, which makes this an interesting comparison.

5.7 Summary

Although there have been many aging tests with drift chambers in the past, there is a lot of variation in the parameters (gas mixture, geometry, materials) of the detectors. This limits the amount of tests whose results could apply to the LHCb OT case.

The COMPASS LAT and ATLAS TRT experiment have performed aging tests with drift chambers constructed with similar materials. Neither the cathode straws nor the glue used was identified as a source of anode wire aging by these experiments. The CMS Muon chamber did suffer from anode aging when an Ar/CO_2 mixture was used, but the anode deposits contained a large amount of silicon. The deposits found on aged wires in the LHCb OT do not contain silicon. This difference between the aging effects makes the addition of CF_4, which is known to prevent silicon deposits, a less viable solution for the LHCb OT. Another problem would be that CF_4 has already been removed from the gas mixture in the LHCb OT, since it caused wire damage. In addition, tests have shown that adding CF_4 does not improve our aging behavior. The strong Malter effect found in the HERA-B OT has not been found in the LHCb OT either, so its solutions do not apply here either.

There have been several reports of aging effects similar to those of the LHCb OT. The CDF COT experienced a gain loss of 50 % after 35 mC/cm, which is comparable to the LHCb OT aging. A SEM picture of a new and aged wire showed a dark, uniform coating on the wire with tiny nodules. This is also similar to the deposits found on wires in the LHCb OT. However, the CDF COT attributes the deposits to the hydrocarbons used in their gas mixture. They specifically suggest that a pure Ar/CO_2 mixture would prevent these results. They did not test this hypothesis. Therefore, their suggested solution of a small oxygen addition could also work for the LHCb OT.

Documentation on aging effects that decreased as the intensity increases is scarce. Most reports on this matter lack sufficient details to be of much use. An experiment for the ATLAS TRT which is described in detail shows several differences with the aging seen in the LHCb OT. The ATLAS TRT group attributes the effect to space charge.

In conclusion, a study of previous experiments did not show an immediately applicable solution to the LHCb OT aging problems. Some suggestions on solving similar problems have been found. Results of testing the space charge hypothesis are shown in chapter 4. The addition of oxygen as a possible solution has also been tested, the results are shown in section 7.4.

Chapter 6

The cause of the aging

Aging tests performed by other experiments, as described in chapter 5, did not find any problems with the materials used in the LHCb OT modules. As such, we cannot be sure which component of the modules causes the aging effects. To investigate this, a special module was constructed. In this chapter the specifications of that module are discussed, and the results of aging tests with this chamber are shown.

6.1 Openable chamber

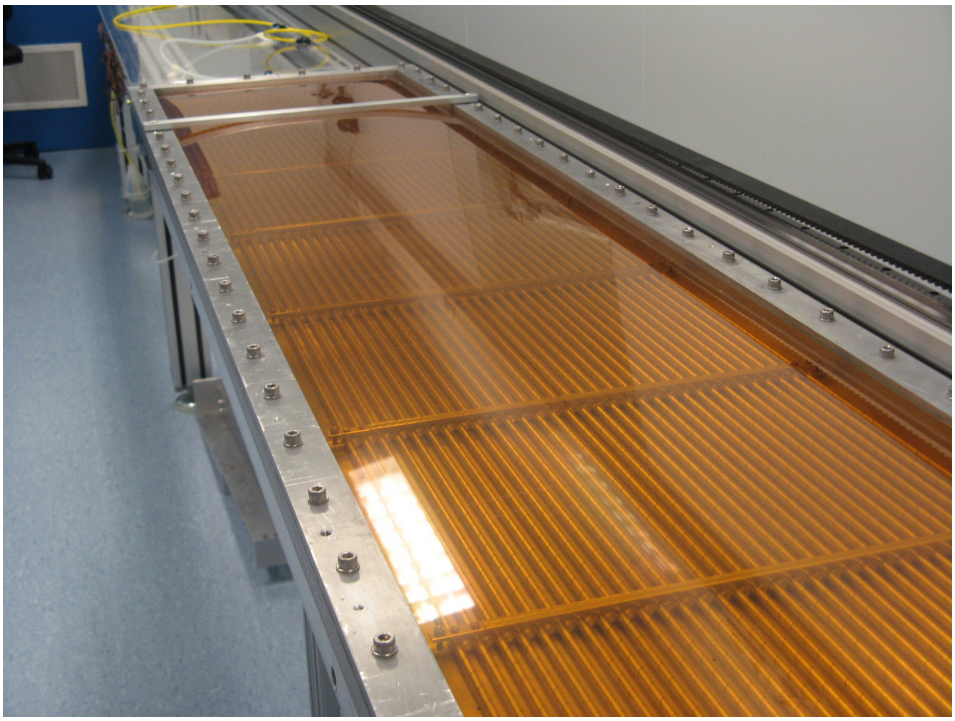

Figure 6.1: *A picture of the openable chamber, module 501.*

The openable chamber, dubbed module 501, was designed to investigate the cause of the aging. This chamber had to be able to operate with as few of the components present in normal modules as possible. It also needed to be easy to open, so those components could be added separately, and so that straws and wires could be removed or replaced as needed.

Figure 6.1 shows a picture of the openable chamber as it has been used in aging tests without added components. It is based on a thick aluminum framework, consisting of two separate parts. The first part is a large aluminum plate. The straws are mounted on top of this plate, using metal clamps. These have the advantage of requiring no glue to keep the straws in place. The drawback is that they are fairly opaque to irradiation, resulting in much lower currents during irradiations at those locations.

The second part is a rectangular frame, with a semi-transparent Kapton foil. The frame can be bolted to the plate, such that the Kapton foil covers the straws. A large O-ring guarantees gas tightness. This creates a gas volume between the aluminum plate and the Kapton. The foil is not very rigid, but it is gas tight. The plate contains the readout system and a gas in- and output.

The Kapton foil covering the module on one side of the module is transparent to radiation, but the aluminum plate is not. The openable chamber is equipped with only one layer of straws, since a second layer of straws between the aluminum plate and the first layer cannot be properly irradiated. The clamps holding the straws in place have room for 64 straws, in the same arrangement as in a F module. However, every other straw holder was left empty, providing 32 straws in total. This provided more room to safely remove straws or wires and allowed us to add straws made with different materials, should there be any indication that the straw material causes the aging (see section 6.2).

The module size, 45x242 cm^2, is similar to an S module. The active area of the straws is about 225 cm in length. The gas volume of the module is relatively large. Since the Kapton foil is not rigid, the gas volume gets inflated when it is connected to the gas input. This provides a large volume outside of the straws, causing a different gas flow inside the straws when the total gas flow is the same as for an F module. Considering the tests shown in section 4.3.3, this difference should be kept in mind.

6.2 Straws and gas mixture

The first tests with the openable chamber were done with as few components as possible. The only components from normal modules present in these tests were the wires, the straws and the electronic readout board. The default gas mixture, 70/30 Ar/CO_2, was used. The openable chamber contained much larger amounts of aluminum than an F module, as well as a large Kapton foil. Neither of these components is expected to significantly alter the aging properties of the detector.

Figure 6.2 shows that a bare module, using the straws and gas mixture of a normal LHCb OT module, suffers no significant aging. Even after 300 hours of

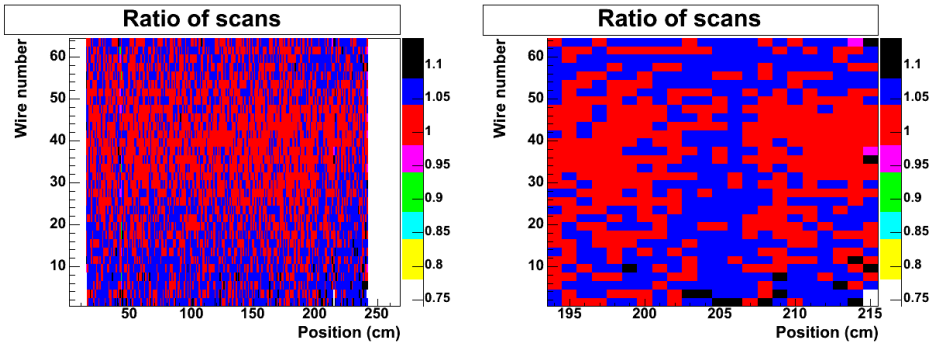

Figure 6.2: *The ratio plots of the openable chamber, after 300 hours of irradiation with the 20 mCi scanning source. The source was placed at 204 cm. The right plot is a zoom of the irradiated area. [Module 501, 18/12/2006 - 02/01/2007]*

irradiation at 204 cm, there is no gain loss visible. Note that the source used in this irradiation is the same source used for scanning. The source profile is not spherically symmetric, and the gain loss caused by this source is usually spread over the full width of the module. In modules that did suffer aging effects, the 20 mCi source quickly caused very large gain losses[1].

We conclude that neither our chosen anode nor cathode material can cause the aging problem that we see in LHCb OT modules. Nor does our chosen gas mixture appear to be the source of the pollutants that cause the aging.

6.3 Panel

The main construction material of normal OT modules is Rohacell foam, coated with a Carbon Fiber Composite (see section 2.2). This material could be a source of the pollutants that cause aging. To test this possibility, a piece of cover material, identical to the material used for the construction of OT modules, was placed within the gas volume. The panel piece, measuring 13 by 110 cm, was placed on top of the straws. It approximately covered wires 40-60, near the gas input, and the Rohacell was in direct contact with the gas, unlike for normal modules.

Figure 6.3 shows the result of irradiating the openable chamber containing the panel piece for 63 hours. The irradiation was performed with the 20 mCi scanning source at position 223. The location of the panel is marked in the left graph by a black rectangle. No significant aging is found. We conclude that the panel material does not cause the aging seen in the LHCb OT.

[1]The lack of aging in the bare openable chamber was confirmed in other irradiations with the usual 2mCi source.

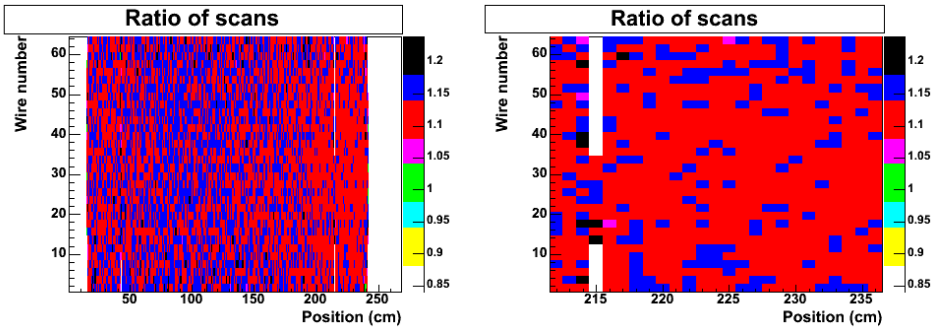

Figure 6.3: *The ratio plots of the openable chamber (similar to Fig. 6.2), after 63 hours of irradiation with the 20 mCi scanning source at 223 cm with a piece of panel in the gas volume. [Module 501, 05/02/2007 - 08/02/2007]*

6.4 Glue

The Araldite AW 103 glue[2] used in the construction of LHCb OT module was considered the most likely source of pollutants. Several test were performed with glue added to the openable chamber. Early tests did not find evidence of aging. However, further tests with glue hardened within the closed module, and irradiations done close to the gas input, did provide compelling evidence that the aging is caused by the Araldite glue.

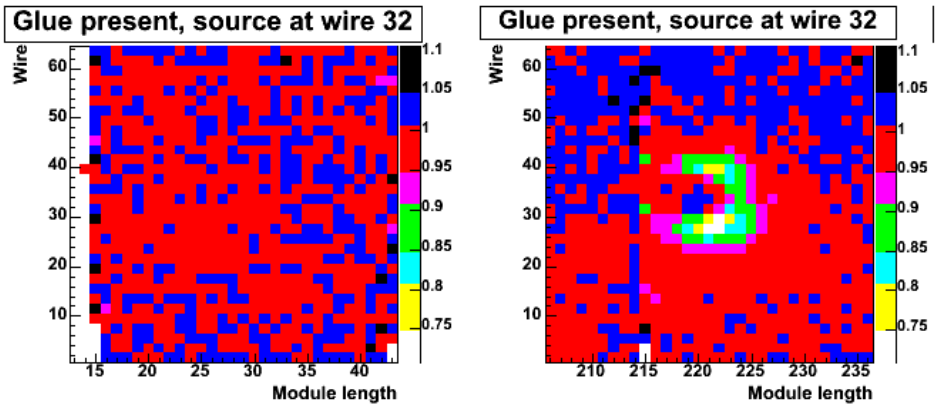

Figure 6.4: *Ratio plots after 20 hour irradiations of module 501 with glue inserted. The gas input is on the right of the module, at 242 cm, and the gas flows from right to left. The left irradiation is done at 28 cm, close to the output. The right irradiation is done at 221 cm, close to the gas input. [Module 501, 03/06/2007 - 06/06/2007]*

Figures 6.4, 6.5 and 6.6 show the results of several irradiations with and without glue inside the detector. In Fig. 6.4, the gas flow is reversed with

[2]Specifically, the glue consists of Araldite AW103 resin, mixed with HY 991 hardener.

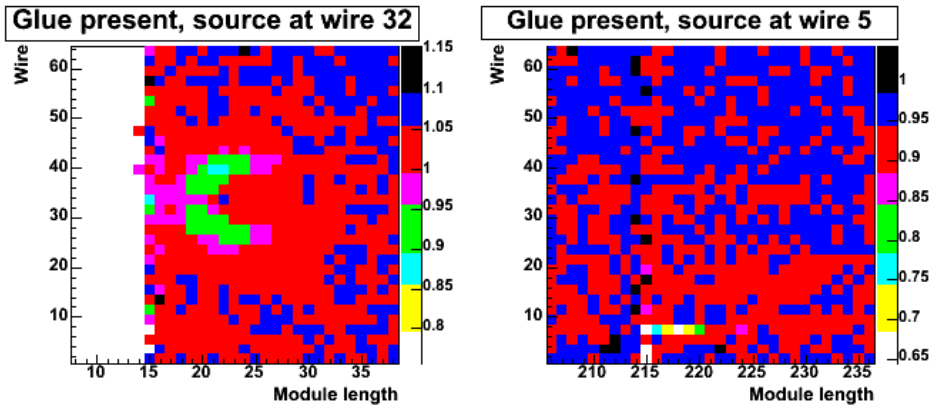

Figure 6.5: *Scans after 20 hour irradiations of module 501 with glue inserted. The gas input is on the left of the module, at 0 cm, and the gas flows from left to right. The left irradiation is done at 23 cm, close to the gas input. The right irradiation is done at 221 cm, close to the gas output. [Module 501, 11/06/2007 - 14/06/2007]*

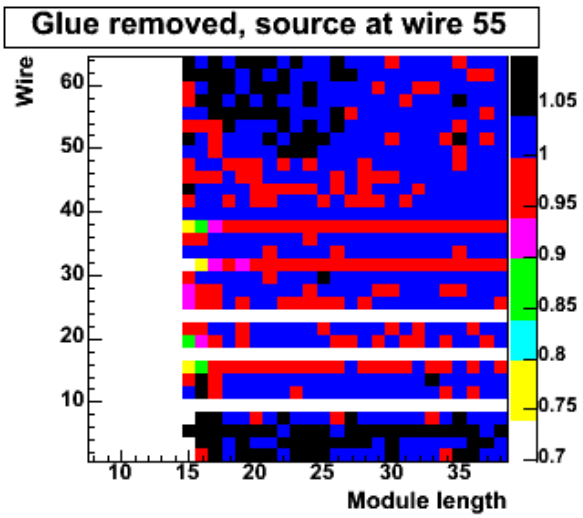

Figure 6.6: *Scans after 115 hours of irradiation of module 501 after the glue had been removed. The gas input is on the left of the module, at 0 cm. The irradiation is done at 23 cm, close to the gas input. [Module 501, 28/06/2007 - 03/07/2007]*

respect to 6.5 and 6.6. Figure 6.6 was made after the glue had been removed from the module. It is immediately apparent that the openable chamber suffers from aging effects identical to the effects seen in LHCb OT modules. The characteristic crescent area of gain loss results from irradiations close to the gas input if glue is present in the module after some 20 hours of irradiation. The much longer irradiation (115 hours) performed without glue does not seem to cause such gain loss. The gain has actually slightly improved at this last irradiation spot[3].

An unusual characteristic of the aging in the openable chamber is that it only seems to occur close to the gas input[4]. This is in contradiction with the results found for an F module in section 4.3.4. The most likely cause for this difference is the gas flow within the straws of the openable chamber. (Tests have shown that the linear gas flow is slower, and the gas front is more smear out when approaching the output, compared to an F module.) However, the large similarities in the aging profile do suggest that the aging effects seen in the openable chamber with glue are identical to those in an LHCb OT module. Therefore, these tests provide sufficient evidence that the Araldite AW 103 glue used in LHCb OT modules is the cause of the aging.

The openable chamber no longer suffers from gain loss after the glue has been removed. This indicates that the pollutants that cause the aging are constantly being emitted by the glue. Once the emission stops, further irradiations cause no gain loss. This is an indication that our problems are caused by outgassing from the glue. Previous experiments (see chapter 5) indicated that Araldite AW 103 is not prone to outgassing. The reasons for this inconsistency are unknown. Finally, if the same glue is placed back in the module after 2 weeks, outgassing appears to have stopped. If outgassing is indeed the cause of the aging effects, heating treatments might be a viable solution to the aging problem. Further details and results of the heating treatments are described in section 7.2.

6.5 Summary

The openable chamber was constructed to investigate the various components used in the LHCB OT modules. By being able to add or remove components, we could determine which component was responsible for the aging effects. Tests show that the used anode, cathode, cover and readout materials do not result in gain loss under irradiation. The Araldite AW 103 glue appears to be the cause of the aging phenomena seen in LHCb OT modules. The test results indicate that the aging is caused by outgassing of pollutants from the glue.

[3] When removing the glue from the openable, several wires broke and were replaced. Some of those new wires showed irregular behavior due to bad wire quality. Three of those wires were disconnected, while two gave excess currents that slowly decreased over time. This is the reason that Fig. 6.6 shows several wires with deviating currents over their entire length. This did not affect the irradiation, as it was performed above wire 55.

[4] Note that both irradiations shown in sections 6.2 and 6.3 were performed close to the gas input as well.

Chapter 7

Solutions

In chapter 6 we have identified the Araldite AW 103 glue as the cause of the observed aging effects. This is useful knowledge when designing new detectors. However, the LHCb OT modules have already been constructed using this glue. We therefore wish to find a procedure that will prevent aging effects in these modules for the duration of the LHCb experiment. Several potential solutions have been investigated: flushing, heating, HV training and adding oxygen.

7.1 Flushing

Section 4.3.4 already showed that the aging rate of a module can decrease over a short period of time. This behavior has been seen with many different modules. However, this only seems to occur if the module is connected to the gas flow[1]. We only notice a decreasing aging rate when the module is being flushed with gas. Presumably, the pollutants emitted by the glue present are transported away by the gas flow. Eventually, the glue will stop emitting pollutants. This hypothesis is supported by aging tests performed with glue in module 501, as described in chapter 6. The fresh glue strips, which caused aging were removed and placed in storage in an open volume. When those strips were placed back in the module, they no longer caused aging. New, 'fresh' glue strips placed in the module did cause aging. It seems that the glue stopped outgassing after exposing the glue to open air.

Figure 7.1 shows the effect on the aging rate of flushing two modules for a long period of time. The aging rate is determined applying the minimum method to 20 hour irradiations with the ^{90}Sr source performed after the specified time of flushing. In both cases the aging rate has a downward trend as a function of flush time (the minimum method results in a value closer to 1), but suffer from occasional 'relapses'. The reason for these dips in the plots are not well understood. Some, but not all, correspond with periods where the module was not connected to the gas flow. Also, several unconnected periods have no effect on the aging rate. For instance, module 3 was unconnected between the last two shown irradiations, but the aging rate is not effected[2].

[1] It need not be the normal Ar/CO_2 gas flow.

[2] Opening the module affects the humidity inside the module. We found no effect of hu-

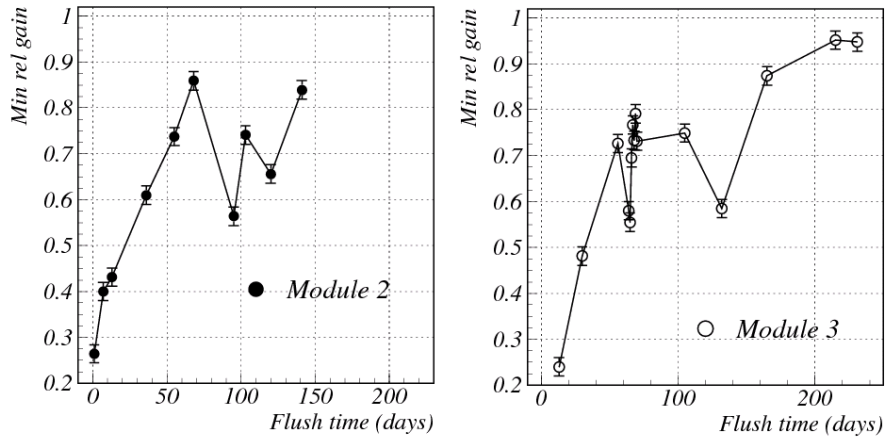

Figure 7.1: *The aging rate, measured with the minimum method, as a function of the flush time for two modules.*

Based on 7.1, we conclude that flushing the modules is beneficial. All modules installed in the LHCb setup at CERN are already being flushed constantly, so this solution is already being applied. However, we do not understand why the aging rate occasionally increases during flushing. Also, the decrease in the aging rate is not large enough to ensure proper operation of the modules for 10 years of LHC run time. Therefore, we wish to find additional ways to reduce or remove the aging effects.

7.2 Heating

Based on the results in chapter 6 and the beneficial effect of flushing shown in section 7.1, we assume that the aging is caused by outgassing from the glue. These outgassing processes generally occur faster at higher temperatures. Therefore, heating a module before irradiation might help to prevent aging effects, because there will be no more pollutants left in the glue that can cause aging during the irradiation. In short, heating the module might provide a faster and more thorough method of achieving the beneficial effects of flushing.

Heating tests performed at the Physikalische Institut in Heidelberg showed promising results [40]. Modules that suffered from normal aging effects after 20 hours of irradiation became very radiation resistant after a heating treatment (see also table 7.2). A first heating test done at NIKHEF in October 2006 was unable to reproduce these results. For all consecutive heating tests, a heating setup closely mimicking the Heidelberg setup was used.

Figure 7.2 shows a picture of the used setup. The module is wrapped in electric blankets. Thin aluminum plates were placed on top of the modules, to improve the heat conduction between the electric blankets and the modules.

midity between 50 and 3000 ppm on the aging. However, the humidity might affect the conductivity of existing deposits.

Figure 7.2: *The setup used for heating modules at NIKHEF.*

The electric blankets were controlled by a computer connected to several temperature sensors placed between the blankets and the module. The computer was set to keep the temperature of the module at 45° C. The module and blankets were wrapped in bubble wrap to insulate the module, making it easier to maintain a fixed temperature. The treated modules were heated for a period of around two weeks each, while flushing the module with CO_2 with 5-10 liter/hr.

Module			Heating	Aging before		Aging after		Result
Origin	Type	No.	date	Min.	Int.	Min.	Int.	
HD	F	192	Mar 07	0.841	-7.9	0.958	-1.4	Much better
NI	F	30	Apr 07	0.650	-10.3	0.703	-9.5	No change
WR	S3	99	May 07	0.328	-40.2	0.398	-28.7	Better
WR	S1	121	Jun 07	0.667	-13.8	0.234	-29.3	Worse
WR	S1	44	Jun 07	0.643	-9.2	0.267	-30.4	Worse

Table 7.1: *Summarized results of heating modules at NIKHEF.*

The results of the heatings with the described setup are summarized in table 7.1. The table lists the location where each module was constructed (NIKHEF, Heidelberg or Warsaw), its identification number and the date at which the heating took place. The results of aging tests performed both before and after the heating procedure are also listed, using both the minimum and the integral quantization method. All these results came from approximately 20 hours of irradiation. Note that the S1 modules 121 and 44 were heated simultaneously. These two modules are only 240 cm long, and were placed in series on the

heating table.

Table 7.1 shows that our heating treatment cannot consistently prevent aging in modules. The heating treatment improved F module 192 and, to a lesser extend, S3 module 99. However, F module 30 was almost unaffected by the heating treatment, and modules 121 and 44 suffered from far more serious aging effects after the heating treatment. Also note that the modules were flushed during the two weeks of heating. In section 7.1 we saw that such a flushing period can improve the aging properties without heating. The improvement in module 99 can be attributed to the flushing time alone. Only the improvement of module 192 is significant.

The differences in the response to the heating treatment are not understood. Modules 121 and 44 were heated simultaneously, and both suffer from similar effects of the heating treatment. This is an indication that the differences are due to differences in the heating treatment. But as these two modules are the only ones that were heated simultaneously with our setup, we cannot yet prove that this is the case. Furthermore, it is not known exactly what the difference between the heating treatments could be. There are no known deviations between the heating of module 192 and 121/44, yet the results vary strongly.

A second possibility is that the deviating results are due to intrinsic properties of the modules. Test have already shown that the aging properties of 'new', unirradiated modules can differ strongly between modules. [3] It is thus possible that the different reactions to heating treatments depend on some unknown difference between the modules. However, the behavior of module 192, which was heated twice (see tables 7.2 and 7.1), leads us to question the hypothesis. This module still suffered from some aging effects after the first heating, but was improved by the second heating. This seems odd if we assume that the success of the heating treatment depends on the module. But the aging properties of this module before the first heating are unknown: it is possible that the first heating actually did improve this module. Therefore, the hypothesis that the heating results depend on the module cannot be proved nor denied with the current data.

Results of heating treatments that were not performed at NIKHEF are shown in tables 7.2 and 7.3. Note that Heidelberg performs aging tests with two ^{55}Fe sources, and uses a different method to quantify the damage. The irradiation damage is shown as the percentage of the gain lost in a ring around the irradiation point. From table 7.2 we see that heating treatments performed at CERN do not yield consistently good results. Module 191 was reasonably resistant to aging after the heating, but all other modules were not. Unfortunately, the aging properties of three of the four tested modules before the heating are unknown. This means we cannot tell if the heating improved those three modules. We can only conclude that the treatments did not always prevent further

[3] When testing modules prior to heating treatments, two S1 modules were found that did not suffer any gain loss after lengthy irradiations. These modules, dubbed 7 and 9, were build in Warsaw, and were similar in all known aspects to modules 121 and 44. Since no aging could be found, heating could not improve these modules further, so modules 7 and 9 were not heated.

Module			Heating		Aging test		
Origin	Type	No.	Location	Date	Before	After	Result
HD	F	191	CERN	Jan 07	Unknown	Good	Unknown
HD	F	192	CERN	Jan 07	Unknown	Poor	Unknown
WR	S1	62-23	CERN	Jan 07	Unknown	Poor	Unknown
NI	F	058	CERN	Jan 07	Poor	Poor	No change
HD	F	170	HD	Oct 06	Poor	Excellent	Much Better

Table 7.2: *Summarized results of heating modules at CERN and Heidelberg, with irradiation tests done at NIKHEF.*

Module		Before			After		
Origin	No.	Irr (hrs)	Irr 1	Irr 2	Irr (hrs)	Irr 1	Irr 2
HD	170	220	28	40	230	4	8
HD	157	160	16	29	186	2	3
HD	177	44	4	4	340	5	5
HD	179	90	12	8	112	<2.5	<2.5
NI	123	115	62	64	110	8	8
NI	005	43	36	34	45	8	9
NI	058	96	3	4	323	3	4
WR	023	96	37	13	90	23	10
WR	S1L	46	50	50	47	30	18

Table 7.3: *Summarized results of heating modules and irradiation tests at Heidelberg. Data from [40].*

aging. Module 58 was tested before the heating treatment. It suffered slightly worse aging effects after the heating at CERN.

In contrast, the heatings performed at Heidelberg usually yield better results, as can be seen in table 7.3. Most modules that suffered from significant aging effects prior to the heating were greatly improved. Most of these modules appear to be sufficiently resistant to radiation to be safely used in the LHCb environment. Only the last two modules showed less significantly improved aging rates. Again, the deviations are not well understood.

In summary, the heating treatment has repeatedly shown promising results in preventing further aging of LHCb OT modules. However, some heating tests resulted in minimal or no improvement, and some heated modules even became more susceptible to aging after the treatment. We have been unable to conclusively identify the difference between heating treatments that had beneficial effects and those that did not. As it stands, heating is a potential solution to the aging problem, but we cannot ensure the beneficial effect for each individual module.

7.3 HV training

Another promising procedure to solve the aging problem is high voltage training. We apply a voltage to all wires that is higher than the 1600 V during normal operation. However, we do not irradiate the module during this treatment. The higher voltage causes currents in the wires even in the absence of a source. We raise the voltage until each wire draws currents in the order of 10 μA. [4] These currents decrease over time while the voltage remains constant. The exact mechanism behind this procedure is unknown. However, tests have shown that this procedure is able of removing gain loss caused by aging, as well as preventing further aging for a period of (usually) 200 hours.

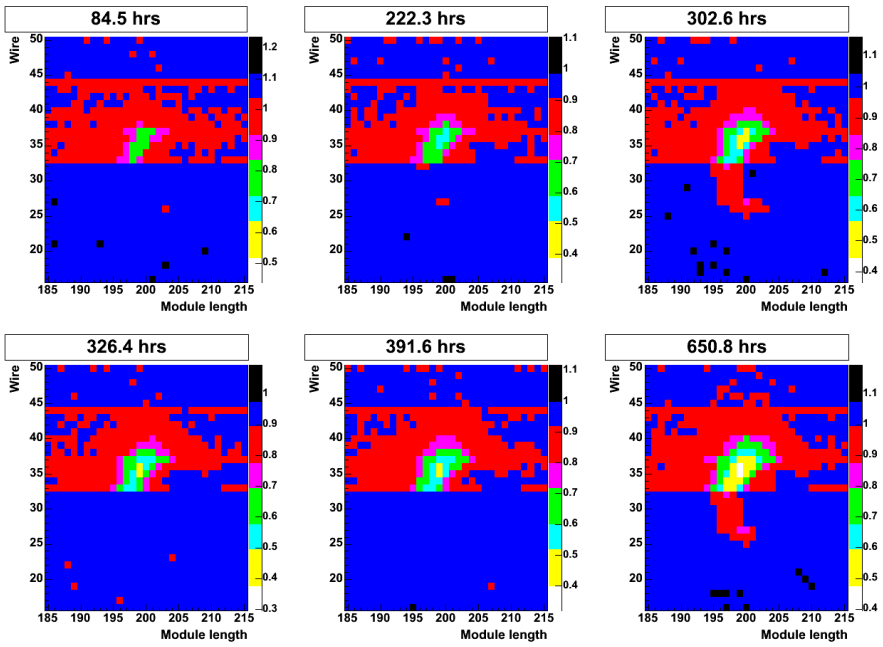

Figure 7.3: *The result of irradiating a module where half of the wires received HV training. The module received HV training a second time after 310 hours of irradiation, after which the gain loss in wires 23-32 disappears. [Module 3 20/08/2006 - 04/10/2006]*

The result of an HV training test are shown in figs 7.3 and 7.4. Wires 1 through 32 were HV trained at 1910 V. Wires 33 through 64 were disconnected during HV training, thus the effects of HV training can be seen by comparing the two halves of the module. Figure 7.3 shows a few of the scans performed during the irradiation. It is immediately apparent that the wires that received HV training age at a much slower rate. After 220 hours of irradiation, the gain loss is still negligible at the trained side. After 300 hours, the trained half also

[4] The exact current is unknown, as our normal current meter cannot measure anything above 500 nA per wire. Instead, we measure the total current of all wires with a less precise current meter.

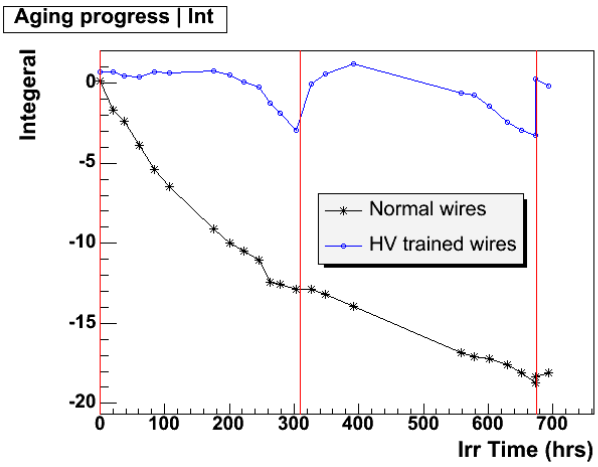

Figure 7.4: *The progress of the aging damage, measured with the integral method, as a function of irradiation time for an HV trained module. The asterisks show the aging of the untrained half, the circles denote the trained half. The vertical lines show the times of the additional HV trainings.*

begins to show gain loss. But after a second HV training after 310 hours, the gain loss at the trained half is reversed. Again, the trained wires age slower than the untrained.

Figure 7.4 shows a summary of the aging, measured with the integral method, during the irradiation. The times of the 3 HV trainings performed (after 0, 310, and 665 hours of irradiation) are marked with vertical lines. The behavior shown in Fig. 7.3 is confirmed by this plot. The gain loss increases normally with the irradiation time at the untrained wires (denoted by the asterisks). The trained wires (circles) show no gain loss for about 200 hours after an HV training. After those 200 hours, the rate of aging is comparable with that of the untrained half at the start of the irradiation. Also, the measured gain loss is removed after each HV training.

It is not known exactly how HV training prevents and cures aging. It is possible that the the high voltage and strong currents during the training either heat the wire or cause discharges which sputter off the deposits on the anode wires. This would explain the reversal of existing gain loss. However, it does not explain why further aging is prevented. In chapter 6 we determined that the glue used in F modules, which is only present outside of the straws, is the cause for the aging. The HV training should only affect the anode wire and the cathode straw. Thus the glue should not be affected by the HV training. A possible explanation would be that the carbon molecules formed under irradiation need some impurities on the wire to condensate on. When the HV training has cleaned the wire of deposits, new deposits may have difficulties attaching themselves to the smooth wire. It would therefore take some time to form new deposits. Once enough of these deposits are formed, new deposits can

condensate at the normal rate. However, this hypothesis cannot be confirmed[5]

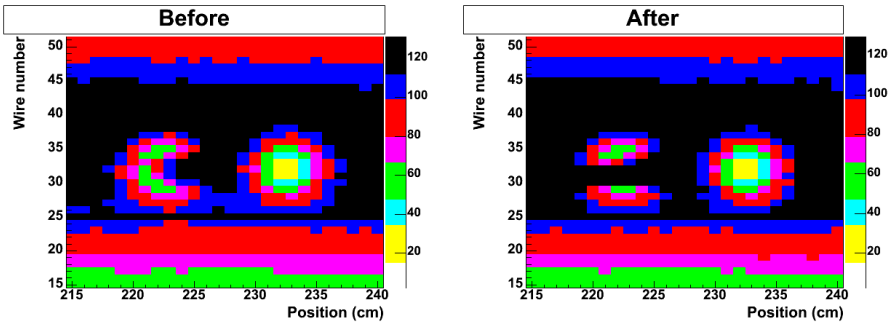

Figure 7.5: *Scans performed before and after a HV training. Only a small part of the gain loss caused by previous irradiations cured. Note that the color scale denotes absolute currents in nA. [Module 121, HV trained at 20/06/2007]*

Several HV training tests have been performed on different modules. The results are not consistently positive. The prevention of new gain loss for a period of time has almost always been observed. However, the removal of previous aging is less consistently observed at all HV trained locations. An example is shown in Fig. 7.5. All wires between 1 and 32 received HV training, but not all of the gain loss caused by previous irradiations was removed. Only in a few wires was the aging reversed, and not at all positions. It is unknown which factors determine if HV training removes the damage.

In an optimal case, HV training can reverse gain loss caused by aging and prevent further aging for 200 hours. The question is how these effects can be properly used to aid the LHCb OT operation. The OT modules must work consistently for 10 years of LHC run time, while HV training prevents aging for about a week. The HV trainings would have to be regularly repeated in order to prevent aging from affecting the detector performance. There may be no significant irradiation during HV training, as the gas gain increases exponentially with the applied high voltage. If the module is irradiated while operating at 1900 V, it will cause too high currents in the wires. Therefore, HV trainings can only be performed during periods where the LHC is shut down.

Based on experiments in plasma physics, it was suggested [41] to attempt a HV training with an oxygen containing gas mixture. So far, only one such test has been done (with a 70/27.5/2.5 $Ar/CO_2/O_2$ gas mixture). Preliminary results of this test showed that some gain loss was removed consistently, at all locations. However, not all gain loss was reversed after one night of HV training. The prevention of new aging lasted for about 100 hours of irradiation in 10 days time.

In summary, HV training is a potential method to remove existing aging effects, while preventing new aging for about a week. It may be useful to reverse

[5]There are also reports (http://physorg.com/news70200836.html) that a rough gold surface could remove oxygen, created by discharges from CO_2, close to the wire by catalyzing the reaction $2CO + O_2 \rightarrow 2CO_2$.

gain loss during downtimes of the LHC, as it requires little preparation or extra infrastructure. However, it is not known if HV trainings can be performed often enough to provide permanent aging prevention on its own. There is insufficient data to determine if HV trainings performed with oxygen yield better results, but preliminary results show no large improvements compared with a normal HV training.

7.4 Oxygen

As mentioned in section 5.5, an aging problem similar to that experienced in the LHCb OT was solved by the addition of oxygen to the gas mixture. In this section we shall show the results of adding oxygen to the LHCb OTs gas mixture.

During our tests, we replaced a small percentage of CO_2 in the usual 70/30 Ar/CO_2 mixture with O_2. It was found that adding oxygen lowers the overall gas gain of the gas mixture. To compensate for this effect, irradiations were performed with a slightly higher applied voltage to increase the gas gain to the original level.

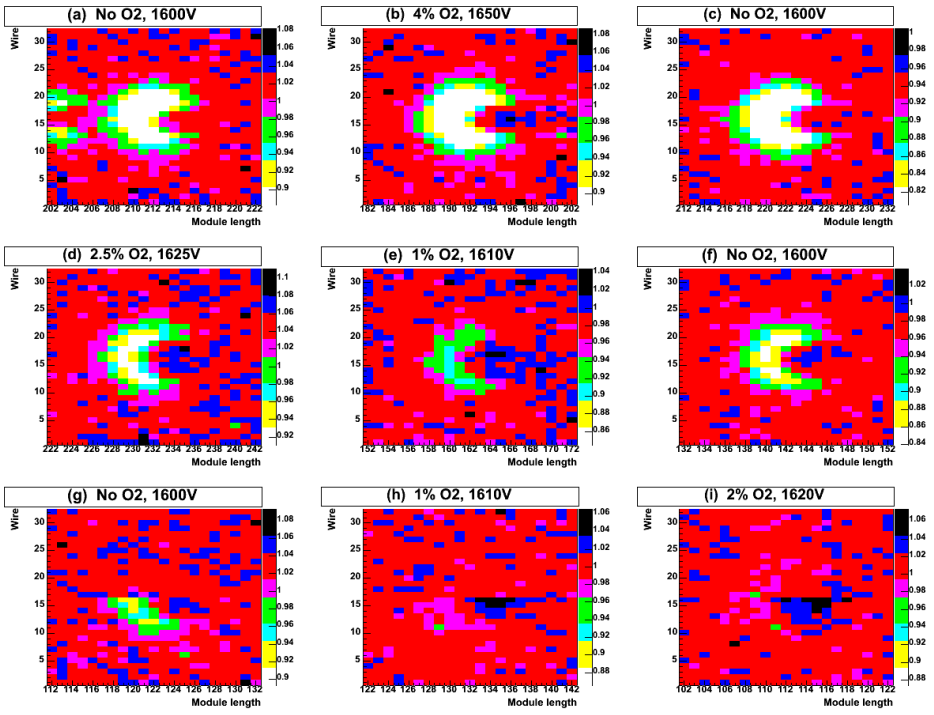

Figure 7.6: *The effects of irradiations with a certain percentage of oxygen in the gas mixture. The irradiations are shown in chronological order. Note that before the irradiation shown in (g) was performed, wires 17-32 received HV training. [Module 99, 05/09/2007 - 10/10/2007]*

Figure 7.6 shows the results of 20 hrs irradiations with the 2mCi source,

with varying amounts of oxygen added to the gas mixture. The irradiations are shown in chronological order. One must keep in mind that later irradiations were performed after a longer flush time. This is most likely largely responsible for the decreasing aging rate observed for irradiations performed without oxygen. From fig 7.6 we see that adding oxygen to the gas mixture can have beneficial effects on the aging rate. However, the amount of oxygen appears to be an important factor. An addition of 4 % oxygen (b) results in an aging rate similar to the aging rate in the normal 70/30 gas mixture (a),(c). A 2.5 % (d) or a 1 % oxygen (e) addition seems to result in a significant improvement in the aging rate. However, part of this improvement might be due to flushing, as can be seen when comparing (c) and (f), which should be identical. But we can confirm that a 1% oxygen addition improves the resistance against aging.

The improvement between 1 % (e) and 2.5 % (d) could either be due to flushing or due to the different percentages. To distinguish between the effects, we also performed these tests in the reversed order, shown in (h) and (i). Note that wires 17-32 received HV training, which affected the aging rate. Consider only wires 1-16. From (h) and (i) we cannot conclude which oxygen percentage results in better aging prevention, as both have similar, low, aging rates.

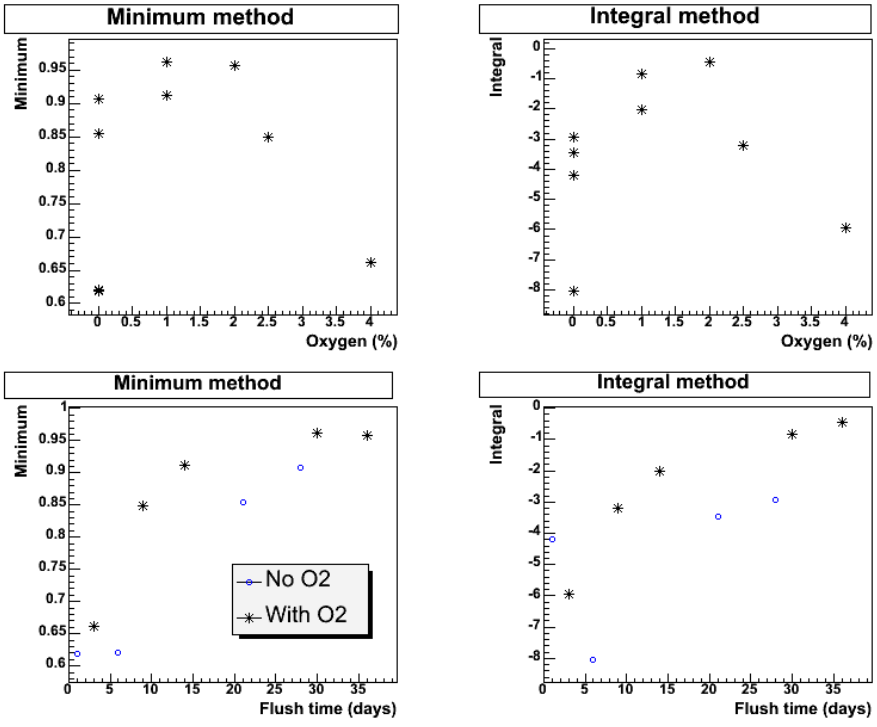

Figure 7.7: *The aging rate, measured with the minimum and integral method, as a function of the oxygen percentage and the flushing time.*

A quantitative summary of the aging rate is shown in Fig. 7.7. The variations (presumably) due to flush time are apparent in the upper two graphs. The lower two graphs confirm that the aging generally decreases with increasing

flushing time. However, these graphs also indicate that the addition of oxygen causes lower aging rates (corresponding to higher values in the graph. Only in the last graph is there one measurement without oxygen (the first one) that results in a lower measured aging rate.

There is currently insufficient data to determine what the optimal oxygen percentage is. We are also unable to reproduce the effects reported by the CDF collaboration, where aging was fully prevented, and old gain loss was reversed. The addition of oxygen only seems to slow the aging progress.

7.5 Summary

Four solutions to the aging problem have been found and tested. Our tests could not prove that any of them will guarantee proper detector operation for the full duration of the experiment.

Flushing appears to have a generally positive effect on the aging rate. However the effect is not expected to be sufficient to guarantee a 10 year detector lifetime. All modules at CERN are already being flushed for about one year. We recommend investigating the current aging rate of some of these modules.

Heating the modules has resulted in very low aging rates in some modules, but we are unable to consistently reproduce this effect. The heatings performed at the Heidelberg institute generally have better results than those performed at NIKHEF, but the cause for this difference in unknown. Currently, the Heidelberg institute is working on a setup to heat all modules in the LHCb OT. The effects of these heatings will be monitored.

HV training is effective in preventing aging for a brief time, and it can also remove old gain loss. If the removal of gain loss can be consistently reproduced, this method could be used to reverse the aging effects during downtimes of the LHC. The power supplies at CERN should suffice to perform HV training on at least part of the modules.

Adding a small oxygen percentage to the gas mixture seems to slow the aging rate. However, the aging rate is still to high to ensure proper detector operation for 10 years. The exact dependence on the oxygen percentage is still unknown.

Perhaps a combination of several methods could solve the aging problem. A long flushing time combined with a small oxygen percentage could slow down the aging process significantly. From Fig. 7.6 we see that about one month of flushing combined with a 1-2 % addition of oxygen greatly reduced the aging rate (from 0.6 to 0.95 with the minimum method). Furthermore, the gas flow in the LHCb setup is currently planned on 10 l/hr, instead of the 20 l/hr in our tests. In section 4.3.3 we showed that this should further lower the aging rate. If necessary, one could investigate if the gas flow can be lowered to 5 l/hr without affecting the detector performance. If the aging rate is lowered sufficiently by these procedures, performing HV trainings during LHC shutdown periods could keep the detectors operational. This possibility should be investigated in greater detail.

Chapter 8

Conclusion

The LHCb OT modules suffers from aging effects, specifically gain loss due to carbon deposits on the anode wire, after short periods of irradiation. No other forms of aging have been observed with our current modules and gas mixture. During a typical irradiation of 20 hours with a 2 mCi ^{90}Sr source a maximum gain loss of 70.000 %/(C/cm) was observed. However, this usual defenition of aging induced gain loss is less useful in our case, because of the unusual intensity dependence that we observed. The area directly below the source, where the irradiation intensity was highest, experienced less aging (2.500 %/(C/cm) in our example) than the fringes of the irradiated area. Furthermore, the area that experiences gain loss is not symmetrical. The area upstream of the irradiated area, with respect to the gas flow, experiences much more aging that the area downstream. Paired with the intensity dependence, this results in a crescent area of gain loss under irradiation with a spherically symmetric source. In contrast, the gain loss has been found to increase with an increasing irradiation time, as would be expected. Since the effects of increasing the intensity and time are different, we conclude that describing the aging in terms of collected charge (intensity times time) is not applicable in our case. Other parameters that determine the aging rate are the gas flow and the flushing time.

The aging effects we observe were unexpected. Aging tests performed prior to construction of the LHCb OT modules showed no aging effects. This could be due to the high intensities used in these accelerated aging tests. Furthermore, other experiments that used similar construction materials and gas mixtures did not report such aging effects. There are few documented cases of lower gain losses at higher intensities, but no literature relevant to our case was found.

In order to identify the cause of the aging, an openable chamber was constructed that could function with a minimal amount of components, and where additional components could be added. Tests with this module show that our chosen gas mixture, straw tubes and panel material do not cause the aging effects. Only when Araldite AW 103 glue is placed in the module do we observe aging effects. These tests indicate that the aging effects are caused by outgassing from the glue.

We have attempted to find a method to reduce the aging rate in the existing LHCb OT modules to the point where we can guarantee that the modules will

suffer no significant gain loss during 10 years of irradiation in the LHC. Several methods were tested, but we have been unable to find a method that suffices. Flushing the modules is a simple procedure, but is not likely to reduce the aging rates sufficiently. Heating the modules has produced some excellent reductions in the aging rate, but we have been unable to consistently reproduce these effects. Several heatings resulted in only slight reduction, no reduction or even an increase of the aging rate. The HV training procedure results in about one week of immunity to aging effects, as well as a removal of previous gain loss. But the immunity period is too short for our purposes, and the gain loss removal cannot be reproduced consistently. Finally, the addition of oxygen has been found to reduce the gain loss by a factor of 2-4, depending on the oxygen concentration. Again, this is insufficient for our purposes.

Further investigation into the aging properties and the outgassing effects of Araldite AW 103 glue might be usefully for future experiments. However, finding a working solution to the aging problem is more urgent, as the aging problem must be solved before the LHC becomes operational. The heating procedure has the greatest potential of preventing aging for 10 years. The heating procedures performed at Heidelberg are generally more successful than the ones performed here at NIKHEF, although the reason is not known. They are currently working on a heating setup that can heat all modules in the LHCb OT stations. The results of this treatment should be monitored.

Furthermore, the installed LHCb OT modules have already been flushed for a year. The aging properties of (some of) these modules will be investigated, to observe if the flushing has resulted in a low aging rate. A scanning setup similar to the those used at NIKHEF is currently being installed at CERN. If needed, a small addition of oxygen could further lower the aging rate. In that case, further investigation in the dependence of the aging rate on the oxygen percentage is recommended. Even then, it might still be necessary to occasionally remove gain loss accumulated during irradiation. The HV training procedure could perform this task, but more tests are necessary to determine why some gain loss is not removed. In short, it should be investigated if a combination of flushing, oxygen and HV trainings during LHC shutdown are sufficient to guarantee a 10 year lifetime of the LHCb OT modules.

In summary, we have been able to determine the cause and several important properties of the aging effects observed in the LHCb OT modules. Unfortunately, we have not yet been able to determine a reliable way to prevent the aging from affecting the performance of existing modules. More research on the potential solutions, or development of new solutions, will be necessary.

Bibliography

[1] P. Lefevre and T. Pettersson, The Large Hadron Collider: conceptual design, CERN-AC-95-05-LHC (1995)

[2] Garwin, R.L., Lederman, L.M., Weinrich, M., Observations of the failure of conservation of parity and charge conjugation in meson decays : the magnetic moment of the free muon, Physical Review, 105(4) (1957) 1415-1417

[3] Wu, C.S., Ambler, E., Hayward, R.W., D.D. Hoppes, and Hudson, R.P., Experimental test of parity conservation in beta decay, Physical Review 105(4) (1957) 1413-1415

[4] J. H. Christenson, J. W. Cronin, V. L. Fitch, and R. Turlay, Evidence for the 2pi Decay of the K20 Meson Physical Review Letters 13 (1964) 138-140

[5] Sakharov, A. D. (1967). "Violation of CP invariance, C asymmetry, and baryon asymmetry of the universe". Soviet Physics Journal of Experimental and Theoretical Physics (JETP) 5: 24-27. Republished in Soviet Physics Uspekhi 34 (1991) 392-393

[6] A. Sanda and I. Bigi, CP Violation, ISBN 0-521-44349-0 (2000)

[7] D. Griffiths, Introduction to Elementary Particles. Wiley, John & Sons, Inc. ISBN 0-471-60386-4 (1987)

[8] B. Aubert et al., Observation of CP violation in the B0 meson system, Physical Review Letters 87:091801 (2001)

[9] K. Abe et al., Observation of large CP violation in the neutral B meson system, Phys.Rev.Lett.87:091802 (2001)

[10] LHCb collaboration, LHCb Reoptimized detector design and performance, CERN-LHCC-2003-030 (2003)

[11] LHCb collaboration, LHCb Outer Tracker Technical Design Report, CERN-LHCC-2001-024 (2001)

[12] R. Fernow, Introduction to experimental particle physics, ISBN 052137940 (1986)

[13] L.B.A Hommels for the LHCb Outer Tracker Collaboration, The LHCb outer tracker detector design and production, CERN-LHCB-2005-014 (2005)

[14] J. Amoraal, Talk at the LHCbweek, (November 2006)

[15] M. Titov, Radiation damage and long-term aging in gas detectors, arXiv:physics/0403055 (2004)

[16] J.Va'vra, Review of Wire Chamber Aging, Nucl. Intsr. and Methods A252 (1986) 547-563

[17] J.A. Kadyk, Wire chamber aging, Nucl. Intsr. and Methods A300 (1991) 436-479

[18] M. Allspach et al., Aging in the Large CDF Axial Drift Chamber,Trans. Nucl. Sci. 52 (2005) 2956-2962

[19] M.Titov et al., Aging studies for the muon detector of HERA-B, Nucl. Intsr. and Methods A515 (2003) 202-219

[20] W.Bonivento et al., Study of ageing side effects in the Delphi HPC calorimeter, Nuclear Physics B (Proc. Suppl.) 54B (1997) 204-209

[21] C. Padilla et al., Aging studies for the large honeycomb drift tube system of the outer tracker of HERA-B, Nucl. Intsr. and Methods A515 (2003) 155-165

[22] R. Christy, Formation of Thin Polymer Films by Electron Bombardment, J. Appl. Phys. 31 (1960) 1680-1683

[23] A. Romaniouk et al., Aging studies for the ATLAS Transition Radiation Tracker (TRT), Nucl. Intsr. and Methods A515 (2003) 166-179

[24] T. Ferguson et al., Aging studies of CMS muon chamber prototypes, Nucl. Intsr. and Methods A488 (2002) 240-257

[25] L. Malter, Thin Film Field Emission, Phys. Rev. 50 (1936) 48-58

[26] S. Bachmann, IEEE2004 NSS-MIC conference (2004)

[27] S. Bachmann, The straw tube technology for the LHCb outer tracking system, Nucl. Intsr. and Methods A535 (2004) 171-174

[28] G. van Apeldoorn et al, Aging studies of straw tube chambers, LHCb-2001-003 (2001)

[29] E. Simioni and Y. Gouz, private communication (2005)

[30] T. Ferguson et al., Gas gain and space charge effects in aging tests of gaseous detectors, Nucl. Intsr. and Methods A515 (2003) 283-287

[31] G. Gavrilov et al., Space distribution of streamers in straw drift tubes, Nucl. Intsr. and Methods A515 (2003) 278-282

[32] ATLAS collaboration, ATLAS Inner Detector Technical design report, CERN/LHCC/97-17 (1997)

[33] T. Akesson et al., Operation of the ATLAS TRT under very high irradiation at the CERN LHC, Nucl. Intsr. and Methods A522 (2004) 25-32

[34] M Capeans, Aging and materials: Lessons for detectors and gas systems, Nucl. Intsr. and Methods A515 (2003) 73-88

[35] COMPASS collaboration, COMPASS: A Proposal for a Common Muon and Proton Apparatus for Structure and Spectroscopy, CERN/SPSLC/96-14, SPSLC/P297 (1996)

[36] V.N. Bychkov, The large size straw drift chambers of the COMPASS experiment, Nucl. Intsr. and Methods A556 (2006) 66-79

[37] J. T. Affolder et al., CDF central outer tracker, Nucl. Intsr. and Methods A526 (2003) 249-299

[38] M. Binkley et al, Aging in large CDF tracking chambers, Nucl. Instr. and Methods A515 (2003) 53-59

[39] CMS collaboration, CMS Muon System Technical design report, CERN/LHCC 97-32 (1997)

[40] T. Haas, PhD thesis, Physikalisches Institut Heidelberg, to be published (2007)

[41] M. Titov, LHCb conference, private communication (2006)